

Lawrence Berkeley National Laboratory

LBL Publications

Title

Standard Model parton distributions at very high energies

Permalink

<https://escholarship.org/uc/item/22b2w87q>

Journal

Journal of High Energy Physics, 2017(8)

ISSN

1126-6708

Authors

Bauer, Christian W
Ferland, Nicolas
Webber, Bryan R

Publication Date

2017-08-01

DOI

10.1007/jhep08(2017)036

Peer reviewed

Standard Model parton distributions at very high energies

Christian W. Bauer,^{a,b} Nicolas Ferland^a and Bryan R. Webber^c

^a*Ernest Orlando Lawrence Berkeley National Laboratory, University of California, Berkeley, CA 94720, U.S.A.*

^b*Theoretical Physics Department, CERN, Geneva, Switzerland*

^c*University of Cambridge, Cavendish Laboratory, J.J. Thomson Avenue, Cambridge, U.K.*

E-mail: cwbauer@lbl.gov, nferland@lbl.gov, webber@hep.phy.cam.ac.uk

ABSTRACT: We compute the leading-order evolution of parton distribution functions for all the Standard Model fermions and bosons up to energy scales far above the electroweak scale, where electroweak symmetry is restored. Our results include the 52 PDFs of the unpolarized proton, evolving according to the SU(3), SU(2), U(1), mixed SU(2)×U(1) and Yukawa interactions. We illustrate the numerical effects on parton distributions at large energies, and show that this can lead to important corrections to parton luminosities at a future 100 TeV collider.

KEYWORDS: Jets, QCD Phenomenology

ARXIV EPRINT: [1703.08562](https://arxiv.org/abs/1703.08562)

Contents

1	Introduction	1
2	The evolution of parton distributions in the full Standard Model	3
2.1	Definition of the parton distribution functions	3
2.2	General evolution equations	6
2.3	Splitting functions	10
2.4	Running couplings	10
2.5	$I = 3$: SU(3) interactions	11
2.6	$I = 1$: U(1) interactions	12
2.7	$I = 2$: SU(2) interactions	13
2.8	$I = Y$: Yukawa interactions	15
2.9	$I = M$: mixed $B - W_3$ interactions	15
3	Implementation details	16
3.1	Switching to a basis of conserved quantum numbers	17
3.2	Cancellation of double-logarithmic dependence in evolution equations	18
4	Results	19
5	Conclusions	26
A	Equations used in the forward evolution	27
A.1	SU(3) interaction	27
A.2	U(1) interaction	27
A.3	SU(2) interaction	28
A.4	Yukawa interaction	29
A.5	Mixed interaction	30

1 Introduction

Experiments at the Large Hadron Collider are now probing the structure of matter at scales comparable with, and even beyond, the characteristic scale of electroweak symmetry breaking. So far, no evidence has been found for a breakdown of the Standard Model (SM) in particle collisions. Indeed, there is a logical possibility that the SM remains a good description of hard scattering processes up to scales far beyond those of any conceivable particle colliders. It is therefore of interest to examine the features predicted by the SM for collider events well above the electroweak scale. For this purpose, Monte Carlo event

generators including all the SM interactions on an equal footing are necessary. Such generators would be useful for investigating the limits of LHC searches, the potential of possible future colliders and cosmic processes at ultrahigh energies.

To construct a general-purpose SM event generator,¹ the three phases of a hard collision, namely initial-state parton showering, parton-parton collision and final-state showering, need to be simulated including all SM particles and interactions. For the initial-state showering, parton distribution functions (PDFs) for all the SM fermions and bosons need to be computed and tabulated beforehand, so that showering can be generated backwards from the hard process, guided by the scale dependence of the PDFs [2, 3].

Recently, a final-state parton shower including emissions from all interactions in the Standard Model was developed [4], which illustrated the importance of electroweak splittings at high energies. For initial-state radiation the generalization of the DGLAP [5–7] evolution equations using all the Standard Model interactions has been worked out in [8], but so far no numerical implementation of these results has been published.

As already mentioned, understanding the DGLAP evolution of PDFs using all interactions of the SM is a required first step in developing a complete initial state parton shower. Moreover, it already allows us to study many new qualitative features of very high-energy processes, such as lepton-initiated processes in hadron collisions and the polarization induced by electroweak PDF evolution.

The inclusion of QED corrections into parton distributions is a well established procedure [9–16]. However, above the electroweak scale around 100 GeV, the contributions of other electroweak bosons become non-negligible and new effects appear [8, 17–30]. PDFs of leptons, vector and scalar bosons are generated dynamically, and left- and right-handed fermions evolve differently. There are also comparable effects in the third generation of quarks due to their Yukawa interactions. Some effects of the SU(2) interaction are double-logarithmically enhanced, due to the non-singlet nature of the incoming states.

The PDF evolution equations for the full Standard Model have been presented in ref. [8]. In the present paper we recast those equations in a form suitable for event generation and solve them numerically for a given set of input distributions at the electroweak scale. The resulting PDF set extends through the region of interest for future colliders and well beyond, so that we can study the onset of the regime where all the SM interactions start to become comparable.

Our solutions to the SM evolution equations are obtained in the approximation of exact SU(3)×SU(2)×U(1) symmetry. That is, we neglect fermion and Higgs masses and the Higgs vacuum expectation value, the effects of these being power-suppressed at high scales. We impose an infra-red cutoff m_V on interactions that involve the emission of an electroweak vector boson, $V = W^i$ for SU(2) or B for U(1). Leading-order evolution kernels and one-loop running couplings are used. All the electroweak PDFs are generated dynamically from the QCD plus photon PDFs, starting from a matching scale $q_0 \sim m_V$. In practice we take $q_0 = m_V = 100$ GeV. In section 4 we show some effects of varying these parameters, to provide an indication of uncertainties due to subleading logarithms and power-suppressed terms.

¹For a review of existing generators, see ref. [1].

For the evolution of the photon, we decompose its PDF into W^3 , B and mixed B/W^3 components at the input scale, evolve these components, and reconstruct the photon PDF from them at higher scales using the running SU(2) and U(1) couplings. For the top quark, we set the PDF to zero below the top mass scale and then use the leading-order massless evolution kernels, as for other fermions. This treatment of the transition region around the electroweak scale is clearly over-simplified but it should give a reliable indication of the magnitude of electroweak effects at higher energies.

The accuracy of our resulting PDFs is leading logarithmic, with subleading logarithmic effects included where possible, but not in a complete way. Contributions to the evolution from the U(1), SU(3) and Yukawa interactions are therefore correct at the single logarithmic level. However, as mentioned above, the SU(2) interactions give rise to double logarithmic effects in the PDF evolution, such that single logarithmic effects in SU(2) non-singlet quantities are not fully under control.

The organization of the paper is as follows. In section 2 we define the relevant parton distribution functions for unpolarized proton beams and the general form of their evolution equations, paying particular attention to the conservation of momentum in the presence of the cutoff m_V for vector boson emission. After specifying all the necessary splitting functions and running couplings, we write the explicit evolution equations associated with the five interactions: SU(3), U(1), SU(2), Yukawa and mixed U(1) \times SU(2), for all the SM partons in a flavor basis. As usual for DGLAP evolution, we do not include 4 point interactions which are suppressed at high energies.

For a numerical implementation, as described in section 3, the flavor basis is not convenient, as too many coupled equations are involved. Instead we use the basis of conserved quantum numbers introduced in ref. [8]. As shown there, the double-logarithmic evolution of SU(2) non-singlet PDFs can then be factored out, which stabilizes and accelerates the solution of the equations. In this way we are able to evolve all the SM PDFs to arbitrarily high scales with satisfactory speed and precision. In practice we evolve up to 10^8 GeV, where the approach to asymptotic behavior is well established.

In section 4, we present a selection of results that illustrate the extent to which electroweak effects change the behavior of the various PDFs. In particular, we show changes in the PDFs of strongly interacting particles relative to pure QCD evolution, and show the size of the PDFs for electroweak gauge bosons relative to the gluon PDF. Finally, we present results of the associated changes in parton-parton luminosities at a 100 TeV pp collider and show the sensitivity of our results to changes of the input values of m_V and q_0 . Our conclusions are presented in section 5.

2 The evolution of parton distributions in the full Standard Model

2.1 Definition of the parton distribution functions

The standard definition of an x -weighted parton distribution is given by the matrix element of a bi-local operator, separated along the lightcone. For fermions, one finds the standard definition, but without spin averaging as we are separating the fermions into left- and

right-handed. Thus, each fermion has only one possible spin determined by its helicity and the sign of its momentum

$$f_i(x, \mu) = x \int \frac{dy}{2\pi} e^{-i2x\bar{n}\cdot py} \langle p | \bar{\psi}^{(i)}(y) \not{\bar{n}} \psi^{(i)}(-y) | p \rangle, \quad (2.1)$$

$$f_{\bar{i}}(x, \mu) = x \int \frac{dy}{2\pi} e^{-i2x\bar{n}\cdot py} \langle p | \psi^{(i)}(y) \not{\bar{n}} \bar{\psi}^{(i)}(-y) | p \rangle, \quad (2.2)$$

where μ is the renormalization scale. Since we have separate left- and right-handed PDFs, for each generation there are a total of 8 quark PDFs and 6 lepton PDFs to consider, giving a total of 42 fermion PDFs.

Parton distributions functions of the vector bosons are given by

$$f_V(x, \mu) = \frac{2}{\bar{n}\cdot p} \int \frac{dy}{2\pi} e^{-i2x\bar{n}\cdot py} \bar{n}_\mu \bar{n}_\nu \langle p | V^{\mu\lambda}(y) V_{\lambda\nu}(-y) | p \rangle \Big|_{\text{spin avg.}}. \quad (2.3)$$

Since SU(3) is unbroken, we consider a single PDF to describe the gluon field. For the SU(2) \otimes U(1) symmetry, on the other hand, one needs to take the symmetry breaking into account. For the W^+ and W^- boson we simply include separate PDFs for each of the two gauge bosons. For the B and W_3 , however, one needs to be more careful to take the mixed contributions of these two bosons into account. Such contributions arise from the fact that the left-handed fermions and Higgs carry both isospin and hypercharge. This implies that besides B and W_3 PDFs one needs to include a mixed PDF, which is given by²

$$f_{BW}(x) = \frac{2}{\bar{n}\cdot p} \int \frac{dy}{2\pi} e^{-i2x\bar{n}\cdot py} \bar{n}^\mu \bar{n}_\nu \langle p | B_{\mu\lambda}(y) W_3^{\lambda\nu}(-y) | p \rangle \Big|_{\text{spin avg.}} + \text{h.c.} \quad (2.4)$$

From these PDFs one can then construct the PDF for the photon, the transversely-polarized Z^0 and their mixed state as a transformation of the PDF for the B , the W_3 and their mixed state. Using $A = c_W B + s_W W_3$ and $Z^0 = -s_W B + c_W W_3$ one finds

$$\begin{pmatrix} f_\gamma \\ f_Z \\ f_{\gamma Z} \end{pmatrix} = \begin{pmatrix} c_W^2 & s_W^2 & c_W s_W \\ s_W^2 & c_W^2 & -c_W s_W \\ -2c_W s_W & 2c_W s_W & c_W^2 - s_W^2 \end{pmatrix} \begin{pmatrix} f_B \\ f_{W_3} \\ f_{BW} \end{pmatrix}, \quad (2.5)$$

and thus

$$\begin{pmatrix} f_B \\ f_{W_3} \\ f_{BW} \end{pmatrix} = \begin{pmatrix} c_W^2 & s_W^2 & -c_W s_W \\ s_W^2 & c_W^2 & c_W s_W \\ 2c_W s_W & -2c_W s_W & c_W^2 - s_W^2 \end{pmatrix} \begin{pmatrix} f_\gamma \\ f_Z \\ f_{\gamma Z} \end{pmatrix}. \quad (2.6)$$

For the electroweak input at scale $\mu = q_0$ we have $f_\gamma(x, q_0) \neq 0$ and $f_Z(x, q_0) = f_{\gamma Z}(x, q_0) = 0$, so the input conditions at that scale are

$$f_B = c_W^2 f_\gamma, \quad f_{W_3} = s_W^2 f_\gamma, \quad f_{BW} = 2c_W s_W f_\gamma. \quad (2.7)$$

²Note that our definition of the mixed PDF f_{BW} is the sum of BW_3 and W_3B contributions, and similarly for the mixed PDF $f_{\gamma Z}$.

where s_W and c_W depend on the value of q of the PDFs

$$s_W \equiv s_W(q) = \sqrt{\frac{\alpha_1(q)}{\alpha_1(q) + \alpha_2(q)}}$$

$$c_W \equiv c_W(q) = \sqrt{\frac{\alpha_2(q)}{\alpha_1(q) + \alpha_2(q)}}. \quad (2.8)$$

Thus, when relating the PDFs at the input scale $\mu = q_0$ in eq. (2.7), one chooses $s_W \equiv s_W(q_0)$ and $c_W \equiv c_W(q_0)$. After evolving these three unbroken PDFs to a higher scale q , the physical photon and Z^0 PDFs are reconstructed using the corresponding running values of $c_W(q)$ and $s_W(q)$.

Finally, one needs to include PDFs for the scalar bosons. One writes

$$f_H(x) = x \int \frac{dy}{2\pi} e^{-i2x\bar{n}\cdot py} \langle p | \Phi(y) \Phi(-y) | p \rangle, \quad (2.9)$$

and PDFs for each of the 4 Higgs fields H^0 , \bar{H}^0 , H^+ and H^- are included. The relationship to the 4 Higgs fields in the unbroken basis to the physical Higgs and the longitudinal gauge bosons is as follows: the H^\pm PDFs correspond to those of the longitudinally polarized W^\pm . In the notation of ref. [8], the neutral Higgs fields are

$$H^0 = \frac{(h - iZ_L)}{\sqrt{2}}, \quad \bar{H}^0 = \frac{(h + iZ_L)}{\sqrt{2}}, \quad (2.10)$$

where h and Z_L represent the Higgs and the longitudinal Z^0 fields, respectively. The corresponding PDFs are

$$f_{H^0} = \frac{1}{2} [f_h + f_{Z_L} + i(f_{hZ_L} - f_{Z_L h})], \quad (2.11)$$

$$f_{\bar{H}^0} = \frac{1}{2} [f_h + f_{Z_L} - i(f_{hZ_L} - f_{Z_L h})], \quad (2.12)$$

and one can also define the mixed PDFs

$$f_{H^0 \bar{H}^0} = \frac{1}{2} [f_h - f_{Z_L} - i(f_{hZ_L} + f_{Z_L h})], \quad (2.13)$$

$$f_{\bar{H}^0 H^0} = \frac{1}{2} [f_h - f_{Z_L} + i(f_{hZ_L} + f_{Z_L h})]. \quad (2.14)$$

Both of these mixed PDF carry non-zero hypercharge, such that they are not produced by the DGLAP evolution in the unbroken gauge theory as considered in this paper.³ Thus, one immediately finds

$$f_h - f_{Z_L} = f_{hZ_L} + f_{Z_L h} = 0, \quad (2.15)$$

and

$$f_h = f_{Z_L} = \frac{1}{2}(f_{H^0} + f_{\bar{H}^0}), \quad f_{hZ_L} = -f_{Z_L h} = -\frac{i}{2}(f_{H^0} - f_{\bar{H}^0}). \quad (2.16)$$

³They are only produced through insertions of the Higgs vacuum.

In summary, there are a total of 52 parton distribution functions that need to be considered. Apart from the QCD quark and gluon distributions, the charged leptons, and the neutral electroweak boson PDFs (2.7), all the other SM PDFs are set to zero at scale q_0 and evolve according to the generalized DGLAP equations presented below.

For the input used here, and because fermion masses and Yukawa couplings are neglected except for the top quark, several fermion PDFs are identical. The lepton PDFs are independent of generation. Also the right-handed fermion and antifermion PDFs are identical, apart from the top quark, unless they are different at the matching scale q_0 . This is the case only for the up and down quarks. The right-handed top and anti-top are slightly different, since they interact through the Yukawa coupling with $H^+ H^-$, respectively. Thus the number of distinct right-handed quark PDFs is reduced from 12 to 9, the left-handed leptons from 12 to 4, and the right-handed leptons from 6 to 1, making a total of 36 non-identical PDFs.

2.2 General evolution equations

We consider the x -weighted PDFs of parton species i at momentum fraction x and scale q , $f_i(x, q)$. In general they satisfy evolution equations of the following forms:

$$\begin{aligned}
 q \frac{\partial}{\partial q} f_i(x, q) &= \sum_I \frac{\alpha_I(q)}{\pi} \left[P_{i,I}^V(q) f_i(x, q) + \sum_j C_{ij,I} \int_x^{z_{\max}^{ij,I}(q)} dz P_{ij,I}^R(z) f_j(x/z, q) \right] \\
 &\equiv \sum_I \left[q \frac{\partial}{\partial q} f_i(x, q) \right]_I .
 \end{aligned}
 \tag{2.17}$$

Here, the sum over I goes over the different interactions in the Standard Model and the notation $[q \partial / \partial q f_i(x, q)]_I$ implies that we only keep the terms proportional to the coupling α_I when taking the derivative.⁴ For the rest of the section, we will show the evolution of each $f_i(x, q)$. We choose $I = 1, 2, 3$ for the pure U(1), SU(2) and SU(3) gauge interactions, $I = Y$ for Yukawa interactions, and $I = M$ for the mixed interaction proportional to

$$\alpha_M(q) = \sqrt{\alpha_1(q) \alpha_2(q)} .
 \tag{2.18}$$

The first contribution, proportional to $P_{i,I}^V$, denotes the virtual contribution to the PDF evolution (the disappearance of a flavor i), while the second contribution is the real contribution (the appearance of flavor i due to the splitting of a flavor j). The maximum value of z in the integration of the real contribution depends on the type of splitting and interaction, and we choose

$$z_{\max}^{ij,I}(q) = \begin{cases} 1 - \frac{m_V}{q} & \text{for } I = 1, 2, \text{ and } i, j \notin V \text{ or } i, j \in V \\ 1 & \text{otherwise} \end{cases} ,
 \tag{2.19}$$

that is, we apply an infrared cutoff m_V , of the order of the electroweak scale, when a B or W boson is emitted. This regulates the divergence of the splitting function for those emissions

⁴Note that $[\dots]_I$ is only introduced for notational convenience and should not be interpreted as setting all other couplings to zero. In particular, the PDFs appearing on the right-hand side of eq. (2.17) still depend on the value of all coupling constants.

$\{\mathbf{T}, \text{CP}\}$	fields
$\{0, +\}$	$2n_g \times q_R, n_g \times \ell_R, n_g \times q_L, n_g \times \ell_L, g, W, B, H$
$\{0, -\}$	$2n_g \times q_R, n_g \times \ell_R, n_g \times q_L, n_g \times \ell_L, H$
$\{1, +\}$	$n_g \times q_L, n_g \times \ell_L, BW, H$
$\{1, -\}$	$n_g \times q_L, n_g \times \ell_L, W, H$
$\{2, +\}$	W

Table 1. The 52 PDFs required for the SM evolution can be written in a basis with definite conserved quantum numbers. $(5n_g + 4)$ PDFs contribute to the $\{0, +\}$ state, $(5n_g + 1)$ to the $\{0, -\}$, $(2n_g + 2)$ to each of the $\{1, +\}$ and $\{1, -\}$ and 1 to the $\{2, +\}$, where $n_g = 3$ stands for number of generations.

as $z \rightarrow 1$. Such a cutoff is mandatory for $I = 2$ because there are PDF contributions that are SU(2) non-singlets. The evolution equations for SU(3) are regular in the absence of a cutoff, as hadron PDFs are color singlets. Similarly for U(1), the unpolarized PDFs have zero hypercharge,⁵ but we include the same cutoff for $I = 1$, since the B and W_3 are mixed in the physical Z and γ states.

Note that the precise choice of the cutoff is somewhat arbitrary, and as already mentioned, we choose $m_V = 100$ GeV in this paper. Changing this value changes our results by subleading logarithmic effect, at the same level as other effects not included. However, given that the SU(2) evolution is double logarithmic, this implies that the ambiguity is single logarithmic for the SU(2) coupling. By matching our results to fixed order, one would account for these terms at first order in α_2 . This is beyond the scope of this paper.

While the flavor basis chosen above is the most intuitive basis, the fact that all 52 PDFs are coupled to one another makes it quite difficult to solve the evolution equations. To decouple some of the equations, it helps to change the basis such that the ingredients have quantum numbers that are conserved in the Standard Model. Choosing the total isospin \mathbf{T} and CP as the quantum numbers, the PDFs for each set of quantum numbers required are shown in table 1.

Note that in general there can be additional mixed PDFs, which however are zero in our initial conditions and which are not generated in the evolution. In particular, there can be states mixing left- and right-handed fermions, but they are not present in the initial condition when only considering unpolarized beams because those states are not Lorentz scalar. Thus, we can drop these states from our evolution.

The sum of momenta of all non-mixed PDFs in the particle basis is conserved, since it is the momentum of the proton. Momentum conservation applies independently for each interaction since physics would still be coherent if we removed one interaction from the Standard Model.

$$\sum_{i \neq \text{BW}} \int_0^1 dx \left[q \frac{\partial}{\partial q} f_i(x, q) \right]_I = 0 \text{ for } I = 1, 2, 3, Y, M. \quad (2.20)$$

⁵Although there can be contributions with non-zero hypercharge for transversely polarized beams [8].

This is equivalent to the sum over all $\mathbf{T} = 0$, $\text{CP} = +$ PDFs in the isospin and CP basis because only these states contribute to a sum over the PDFs in the particle basis. For the other values of \mathbf{T} and CP, the PDFs correspond to differences of PDFs in the particle basis. For example an isospin 1 PDF is added in PDF of an up-type fermion, but subtracted in the down-type PDF, thus it has no effect on the sum.

Combining eqs. (2.17) and (2.20) gives

$$\begin{aligned}
0 &= \sum_{i \neq \text{BW}} P_{i,I}^V \int_0^1 dx f_i(x, q) + \sum_{i,j} C_{ij,I} \int_0^1 dx \int_x^{z_{\max}^{ij,I}(q)} dz P_{ij,I}^R(z) f_j(x/z, q) \\
&= \sum_{i \neq \text{BW}} P_{i,I}^V \int_0^1 dx f_i(x, q) + \sum_{i,j} C_{ij,I} \int_0^{z_{\max}^{ij,I}(q)} dz P_{ij,I}^R(z) \int_0^z dx f_j(x/z, q) \\
&= \sum_{i \neq \text{BW}} P_{i,I}^V \langle f_i(q) \rangle + \sum_{i,j} C_{ij,I} \int_0^{z_{\max}^{ij,I}(q)} z dz P_{ij,I}^R(z) \langle f_j(q) \rangle, \tag{2.21}
\end{aligned}$$

where we have defined the momentum averaged PDF

$$\langle f_i(q) \rangle \equiv \int_0^1 dx f_i(x, q). \tag{2.22}$$

Solving the equation for each of the $\langle f_i(q) \rangle$, since all the input particle PDFs can be set independently, we get

$$P_{i,I}^V(q) = - \sum_j C_{ji,I} \int_0^{z_{\max}^{ji,I}(q)} z dz P_{ji,I}^R(z) \text{ for } i \neq \text{BW}. \tag{2.23}$$

Thus, momentum conservation determines the factor $P_{i,I}^V$ for all non-mixed fields in the particle basis.

Note that the result from momentum conservation agrees up to power corrections with the more traditional definition of the virtual corrections as loop insertions on the fields of the PDF, which we denote by $\tilde{P}_{i,I}^V$. Summing over possible loops, one has

$$\begin{aligned}
\tilde{P}_{f_i,I}^V(q) &= -C_{ff,i,I} \int_0^{z_{\max}^{ff,I}(q)} dz P_{ff,I}^R(z) \\
\tilde{P}_{V_i,I}^V(q) &= -\frac{C_{VV,i,I}}{2} \int_0^{z_{\max}^{VV,I}(q)} dz P_{VV,I}^R(z) - \sum_{j \in f,h} C_{jV_i,I} \int_0^1 dz P_{jV,I}^R(z) \\
\tilde{P}_{H_i,I}^V(q) &= -C_{HH,i,I} \int_0^{z_{\max}^{HH,I}(q)} dz P_{HH,I}^R(z) - \sum_{j \in f} C_{jH_i,I} \int_0^1 dz P_{jH,I}^R(z), \tag{2.24}
\end{aligned}$$

where $\sum_{j \in f,h}$ is a sum over all fermions and Higgs bosons which are not antiparticles, and

$$C_{ff,i,I} = \sum_j C_{jf_i,I} \tag{2.25}$$

and similarly for $C_{VV,i,I}$ and $C_{HH,i,I}$. To see that eqs. (2.23) and (2.24) agree with each other, we will work it out explicitly for the virtual contribution to a fermion. One uses for the fermions that $P_{Vf,I}^R(z) = P_{ff,I}^R(1-z)$ and $C_{ff,I} = C_{Vf,I}$ to obtain the correct relation:

$$\begin{aligned} P_{f,I}^V(q) &= -C_{ff,I} \left[\int_0^{z_{\max}} z \, dz P_{ff,I}^R(z) + \int_0^1 z \, dz P_{Vf,I}^R(z) \right] \\ &= -C_{ff,I} \left[\int_0^{z_{\max}} z \, dz P_{ff,I}^R(z) + \int_0^1 (1-z) \, dz P_{ff,I}^R(z) \right] \\ &= \tilde{P}_{f,I}^V(q) + \dots, \end{aligned} \tag{2.26}$$

where \dots denotes power corrections in $1 - z_{\max}$. The argument is exactly the same for $P_{H,I}^V(q)$, while for $P_{V,I}^V(q)$ one simply uses that $P_{VV,I}^R(z)$ and $P_{fV,I}^R(z)$, and $P_{hV,I}^R(z)$ and $P_{fH,I}^R(z)$, are symmetric in $z \leftrightarrow 1-z$ to write $\int z \, dz = \int dz/2$. In our implementation of the evolution equations, we use eq. (2.23), to ensure exact momentum conservation without explicit power corrections.

Since the mixed PDF f_{BW} is a pure $\mathbf{T} = 1$ state, it does not contribute to the momentum sum. This implies that one cannot derive its associated virtual contribution from momentum conservation. However, using the traditional definition in terms of loops, one sees that in this case the U(1) and SU(2) virtual corrections each apply to only one of the two fields involved, and therefore

$$\tilde{P}_{BW,1}^V(q) = \frac{1}{2} P_{B,1}^V(q), \quad \tilde{P}_{BW,2}^V(q) = \frac{1}{2} P_{W,2}^V(q), \tag{2.27}$$

while the virtual contribution is zero for the other interactions.

One can simplify the general evolution equations in eq. (2.17) by defining a full Sudakov factor

$$\Delta_i(q) = \exp \left[\sum_I \int_{q_0}^q \frac{dq'}{q'} \frac{\alpha_I(q')}{\pi} P_{i,I}^V(q') \right], \tag{2.28}$$

as well as a partial Sudakov factor for each interaction

$$\Delta_{i,I}(q) = \exp \left[\int_{q_0}^q \frac{dq'}{q'} \frac{\alpha_I(q')}{\pi} P_{i,I}^V(q') \right], \tag{2.29}$$

where q_0 is an arbitrary cutoff, which for convenience we set equal to m_V . This allows us to write

$$\left[\Delta_{i,I}(q) q \frac{\partial}{\partial q} \frac{f_i(x, q)}{\Delta_{i,I}(q)} \right]_I = \frac{\alpha_I(q)}{\pi} \sum_j C_{ij,I} P_{ij,I}^R \otimes f_j, \tag{2.30}$$

where again the notation $[\dots]_I$ implies that only terms from the interaction I are kept. This gives

$$\begin{aligned} \Delta_i(q) q \frac{\partial}{\partial q} \left[\frac{f_i(x, q)}{\Delta_i(q)} \right] &= \sum_I \left[\Delta_{i,I}(q) q \frac{\partial}{\partial q} \frac{f_i(x, q)}{\Delta_{i,I}(q)} \right]_I \\ &= \sum_I \frac{\alpha_I(q)}{\pi} \sum_j C_{ij,I} P_{ij,I}^R \otimes f_j, \end{aligned} \tag{2.31}$$

where

$$P_{ij,I}^R \otimes f_j \equiv \int_x^{z_{\max}^{ij,I}(q)} dz P_{ij,I}^R(z) f_j(x/z, q). \tag{2.32}$$

2.3 Splitting functions

The splitting functions depend only on the type of particles, which for the Standard Model are the spin 1/2 fermions, denoted by f , spin 1 gauge bosons, denoted by V , as well as spin 0 Higgs bosons, denoted by H .

Denoting the three gauge interactions of the Standard Model collectively by $I = G$, the splitting functions involving gauge bosons are given by

$$P_{ff,G}^R(z) = \frac{1+z^2}{1-z}, \quad (2.33)$$

$$P_{Vf,G}^R(z) = P_{ff,G}(1-z), \quad (2.34)$$

$$P_{fV,G}^R(z) = \frac{1}{2} [z^2 + (1-z)^2], \quad (2.35)$$

$$P_{VV,G}^R(z) = 2 \left[\frac{z}{1-z} + \frac{1-z}{z} + z(1-z) \right] \quad (2.36)$$

$$P_{HH,G}^R(z) = \frac{2z}{1-z}, \quad (2.37)$$

$$P_{VH,G}^R(z) = P_{HH,G}^R(1-z), \quad (2.38)$$

$$P_{HV,G}^R(z) = z(1-z). \quad (2.39)$$

The factor of 1/2 in P_{fV} has to be included since we are considering fermions with definite chirality. For the Yukawa interaction (Y), one obtains

$$P_{ff,Y}^R(z) = \frac{1-z}{2}, \quad (2.40)$$

$$P_{Hf,Y}^R(z) = P_{ff,Y}^R(1-z), \quad (2.41)$$

$$P_{fH,Y}^R(z) = \frac{1}{2}. \quad (2.42)$$

2.4 Running couplings

The one-loop running of the gauge couplings α_I ($I = 1, 2, 3$) is given by

$$\frac{2\pi}{\alpha_I(q_2)} = \frac{2\pi}{\alpha_I(q_1)} + \beta_I \ln \frac{q_2}{q_1}, \quad (2.43)$$

where, for n_g generations and n_H Higgs doublets,

$$\beta_1 = -\frac{1}{3}\rho_1 = -\frac{20}{9}n_g - \frac{1}{6}n_H = -\frac{41}{6}, \quad (2.44)$$

$$\beta_2 = \frac{2}{3}(11 - \rho_{V2}) = \frac{22}{3} - \frac{4}{3}n_g - \frac{1}{6}n_H = \frac{19}{6}, \quad (2.45)$$

$$\beta_3 = 11 - \rho_3 = 11 - \frac{4}{3}n_g = 7. \quad (2.46)$$

At scale $M_Z = 91.2 \text{ GeV}$ we take

$$\sin^2 \theta_W = \frac{\alpha_1}{\alpha_1 + \alpha_2} = 0.23, \quad \alpha = \alpha_2 \sin^2 \theta_W = \frac{1}{128}, \quad \alpha_3 = 0.118, \quad (2.47)$$

which gives

$$\alpha_1(M_Z) = 0.0101 \quad \alpha_2(M_Z) = 0.0340 \quad \alpha_3(M_Z) = 0.118. \quad (2.48)$$

We set all Yukawa couplings to zero, except for the top Yukawa coupling $\alpha_Y = y_t^2/4\pi$. Its running receives significant Yukawa and QCD contributions:

$$q \frac{\partial \alpha_Y}{\partial q} = \frac{\alpha_Y}{2\pi} (\beta_Y \alpha_Y - \beta_S \alpha_3), \quad (2.49)$$

where $\beta_Y = 9/2$ and $\beta_S = 8$. The solution is

$$\frac{1}{\alpha_Y(q_2)} = \frac{\delta}{\alpha_3(q_2)} - \left[\frac{\delta}{\alpha_3(q_1)} - \frac{1}{\alpha_Y(q_1)} \right] \left[\frac{\alpha_3(q_1)}{\alpha_3(q_2)} \right]^\gamma, \quad (2.50)$$

where

$$\gamma = \frac{\beta_S}{\beta_3} = \frac{24}{33 - 4n_g} = \frac{8}{7}, \quad (2.51)$$

$$\delta = \frac{\beta_Y}{\beta_S - \beta_3} = \frac{27}{8n_g - 18} = \frac{9}{2}. \quad (2.52)$$

We take $m_t(m_t) = 163$ GeV, which implies $\alpha_Y(m_t) = 0.0349$, and $\alpha_3(m_t) = 0.109$.

2.5 $I = 3$: SU(3) interactions

We start by considering the well known case of SU(3) interactions. The relevant degrees of freedom are the gluon, as well as left and right-handed quarks. The coupling constants are (with $C_F = 4/3$, $C_A = 3$, $T_R = 1/2$)

$$C_{qq,3} = C_{gq,3} = C_F, \quad C_{qg,3} = T_R, \quad C_{gg,3} = C_A. \quad (2.53)$$

This gives for the evolution of a quark or gluon⁶

$$\left[\Delta_{q,3} q \frac{\partial}{\partial q} \frac{f_q}{\Delta_{q,3}} \right]_3 = \frac{\alpha_3}{\pi} [C_F P_{ff,G}^R \otimes f_q + T_R P_{fV,G}^R \otimes f_g], \quad (2.54)$$

$$\left[\Delta_{g,3} q \frac{\partial}{\partial q} \frac{f_g}{\Delta_{g,3}} \right]_3 = \frac{\alpha_3}{\pi} \left[C_A P_{VV,G}^R \otimes f_g + \sum_f C_F P_{fV,G}^R \otimes f_q \right]. \quad (2.55)$$

The Sudakov factor can be obtained from eq. (2.23) using the coupling constants in eq. (2.53). This gives

$$P_{q,3}^V(q) = -C_F \int_0^1 z dz [P_{ff,G}^R(z) + P_{fV,G}^R(z)], \quad (2.56)$$

$$P_{g,3}^V(q) = - \int_0^1 z dz [C_A P_{VV,G}^R(z) + 8 n_g T_R P_{fV,G}^R(z)], \quad (2.57)$$

where we have used in the last line that there are 8 chiral quarks plus antiquarks per generation.

⁶From now on we omit the arguments of functions for brevity.

Since the gluon is massless, the upper limit in all the z integrations is equal to 1 [see eq. (2.19)]. This implies that the convolutions $P_{ff,G}^R \otimes f_q$ and $P_{VV,G}^R \otimes f_g$ in eqs. (2.54) and (2.55) are both divergent. However, at the same time the virtual splitting functions that enter the Sudakov factors $\Delta_{q,3}(q)$ and $\Delta_{g,3}(q)$ defined in eq. (2.29) are also divergent, such that the divergences cancel in the evolution of the actual PDFs. Using +-distributions, as explained in section 3, one obtains evolution equations that are free of any divergences, and which can be implemented numerically. Alternatively, for parton shower implementation, one can impose a cutoff of the form eq. (2.19) with m_V replaced by a small parameter $m_g > \Lambda_{\text{QCD}}$.

2.6 $I = 1$: U(1) interactions

For U(1) the relevant degrees of freedom are left- and right-handed fermions (denoted by the subscript f), as well as the U(1) gauge boson B . The couplings involving fermions and gauge bosons are

$$C_{ff,1} = C_{Bf,1} = Y_f^2, \quad C_{fB,1} = N_f Y_f^2, \quad C_{BB,1} = 0 \quad (2.58)$$

where the hypercharges of the different fermions are given by

$$Y_{q_L} = \frac{1}{6}, \quad Y_{u_R} = \frac{2}{3}, \quad Y_{d_R} = -\frac{1}{3}, \quad Y_{\ell_L} = -\frac{1}{2}, \quad Y_{e_R} = -1, \quad (2.59)$$

and the color factor N_f is equal to 3 for quarks and 1 for leptons. The couplings involving the Higgs bosons are

$$C_{hh,1} = C_{Bh,1} = C_{hB,1} = \frac{1}{4}, \quad (2.60)$$

where h here stands for any of the four Higgs boson PDFs.

Plugging this into the general evolution equation gives

$$\left[\Delta_{f,1} q \frac{\partial}{\partial q} \frac{f_f}{\Delta_{f,1}} \right]_1 = \frac{\alpha_1}{\pi} Y_f^2 [P_{ff,G}^R \otimes f_f + N_f P_{fV,G}^R \otimes f_B], \quad (2.61)$$

$$\left[\Delta_{B,1} q \frac{\partial}{\partial q} \frac{f_B}{\Delta_{B,1}} \right]_1 = \frac{\alpha_1}{\pi} \left[\sum_f Y_f^2 P_{Vf,G}^R \otimes f_f + \frac{1}{4} \sum_h P_{VH,G}^R \otimes f_h \right], \quad (2.62)$$

$$\left[\Delta_{H,1} q \frac{\partial}{\partial q} \frac{f_h}{\Delta_{H,1}} \right]_1 = \frac{\alpha_1}{\pi} \frac{1}{4} [P_{HH,G}^R \otimes f_h + P_{HV,G}^R \otimes f_B]. \quad (2.63)$$

The virtual splitting functions, required for the Sudakov factor are given by

$$P_{f,1}^V(q) = -Y_f^2 \left[\int_0^{1-\frac{m_V}{q}} z dz P_{ff,G}^R(z) + \int_0^1 z dz P_{Vf,G}^R(z) \right], \quad (2.64)$$

$$P_{B,1}^V(q) = -n_g \left(\frac{11}{9} N_C + 3 \right) \int_0^1 z dz P_{fV,G}^R(z) - \int_0^1 z dz P_{HV,G}^R(z), \quad (2.65)$$

$$P_{H,1}^V(q) = -\frac{1}{4} \left[\int_0^{1-\frac{m_V}{q}} z dz P_{HH,G}^R(z) + \int_0^1 z dz P_{VH,G}^R(z) \right], \quad (2.66)$$

where we have used in the second line that for each generation there are 4 left-handed quarks (one needs to count particles and antiparticles separately), 2 right-handed up-type quarks, 2 right-handed down-type quarks, 4 left-handed leptons and 2 right-handed electrons, and that there are a total of 4 Higgs bosons.

2.7 $I = 2$: SU(2) interactions

The SU(2) interactions are more complicated, since the emission of W^\pm bosons changes the flavor of the emitting particle. This, combined with the SU(2) breaking in the input hadron PDFs, leads to double-logarithmic scale dependence in the DGLAP evolution, rather than only single-logarithmic dependence as in the evolution based on U(1) and SU(3).

The relevant coupling constants are (where u_L and d_L denote any up- and down-type left-handed fermion)

$$C_{u_L d_L,2} = C_{d_L u_L,2} = C_{W^+ u_L,2} = C_{W^- d_L,2} = \frac{1}{2}, \quad (2.67)$$

$$C_{u_L u_L,2} = C_{W_3 u_L,2} = C_{d_L d_L,2} = C_{W_3 d_L,2} = \frac{1}{4}, \quad (2.68)$$

$$C_{u_L W^+,2} = C_{d_L W^-,2} = N_f \frac{1}{2}, \quad (2.69)$$

$$C_{u_L W_3,2} = C_{d_L W_3,2} = N_f \frac{1}{4}, \quad (2.70)$$

$$C_{W^\pm W^\pm,2} = C_{W^\pm W_3,2} = C_{W_3 W^\pm,2} = 1, \quad (2.71)$$

where as before the color factor $N_f = 3$ for quarks, 1 for leptons. The couplings of the W_3 state to the Higgs are given by

$$C_{hh,2} = C_{W_3 h,2} = C_{h W_3,2} = \frac{1}{4}, \quad (2.72)$$

where again h stands for any of the 4 Higgs bosons, while those of the charged W states are given by

$$\begin{aligned} C_{H^+ H^0,2} &= C_{H^0 H^+,2} = C_{H^+ W^+,2} = C_{W^+ H^+,2} \\ &= C_{H^0 W^-,2} = C_{W^- H^0,2} = \frac{1}{2}. \end{aligned} \quad (2.73)$$

The couplings for the charge-conjugate states are the same.

This gives for the evolution of the fermions

$$\begin{aligned} \left[\Delta_{f_L,2} q \frac{\partial}{\partial q} \frac{f_{u_L}}{\Delta_{f_L,2}} \right]_2 &= \frac{\alpha_2}{\pi} \left\{ P_{ff,G}^R \otimes \left[\frac{f_{d_L}}{2} + \frac{f_{u_L}}{4} \right] \right. \\ &\quad \left. + N_f P_{fV,G} \otimes \left[\frac{f_{W^+}}{2} + \frac{f_{W_3}}{4} \right] \right\}, \end{aligned} \quad (2.74)$$

$$\begin{aligned} \left[\Delta_{f_L,2} q \frac{\partial}{\partial q} \frac{f_{d_L}}{\Delta_{f_L,2}} \right]_2 &= \frac{\alpha_2}{\pi} \left\{ P_{ff,G}^R \otimes \left[\frac{f_{u_L}}{2} + \frac{f_{d_L}}{4} \right] \right. \\ &\quad \left. + N_f P_{fV,G} \otimes \left[\frac{f_{W^-}}{2} + \frac{f_{W_3}}{4} \right] \right\}. \end{aligned} \quad (2.75)$$

For the W^+ and W_3 bosons we have

$$\left[\Delta_{W,2} q \frac{\partial}{\partial q} \frac{f_{W^+}}{\Delta_{W,2}} \right]_2 = \frac{\alpha_2}{\pi} \left\{ P_{VV,G}^R \otimes [f_{W^+} + f_{W_3}] + \frac{1}{2} P_{VH,G}^R \otimes [f_{H^+} + f_{\bar{H}^0}] \right. \\ \left. + \sum_{\text{gen}} \frac{1}{2} P_{Vf,G}^R \otimes [f_{u_L} + f_{\bar{d}_L} + f_{\nu_L} + f_{\bar{\ell}_L}] \right\}, \quad (2.76)$$

$$\left[\Delta_{W,2} q \frac{\partial}{\partial q} \frac{f_{W_3}}{\Delta_{W,2}} \right]_2 = \frac{\alpha_2}{\pi} \left\{ P_{VV,G}^R \otimes [f_{W^+} + f_{W^-}] + \frac{1}{4} P_{VH,G}^R \otimes \sum_h f_h \right. \\ \left. + \frac{1}{4} \sum_{f_L} P_{Vf,G}^R \otimes f_{f_L} \right\}, \quad (2.77)$$

where the sum in the last line is over all left-handed fermions and anti-fermions. The equation for the W^- can be obtained from that of the W^+ by charge conjugation.

Finally, for the Higgs bosons we have

$$\left[\Delta_{H,2} q \frac{\partial}{\partial q} \frac{f_{H^+}}{\Delta_{H,2}} \right]_2 = \frac{\alpha_2}{\pi} \left\{ P_{HH,G}^R \otimes \left[\frac{f_{H^0}}{2} + \frac{f_{H^+}}{4} \right] \right. \\ \left. + P_{HV,G} \otimes \left[\frac{f_{W^+}}{2} + \frac{f_{W_3}}{4} \right] \right\}, \quad (2.78)$$

$$\left[\Delta_{H,2} q \frac{\partial}{\partial q} \frac{f_{H^0}}{\Delta_{H,2}} \right]_2 = \frac{\alpha_2}{\pi} \left\{ P_{HH,G}^R \otimes \left[\frac{f_{H^+}}{2} + \frac{f_{H^0}}{4} \right] \right. \\ \left. + P_{HV,G} \otimes \left[\frac{f_{W^-}}{2} + \frac{f_{W_3}}{4} \right] \right\}. \quad (2.79)$$

The virtual splitting functions are

$$P_{f,2}^V(q) = -\frac{3}{4} \left[\int_0^{1-\frac{m_V}{q}} z \, dz P_{ff,G}^R(z) + \int_0^1 z \, dz P_{Vf,G}^R(z) \right], \quad (2.80)$$

$$P_{W,2}^V(q) = -2 \int_0^{1-\frac{m_V}{q}} z \, dz P_{VV,G}^R(z) - n_g(N_C + 1) \int_0^1 z \, dz P_{fV,G}^R(z) - \int_0^1 z \, dz P_{HV,G}^R(z), \quad (2.81)$$

$$P_{H,2}^V(q) = -\frac{3}{4} \left[\int_0^{1-\frac{m_V}{q}} z \, dz P_{HH,G}^R(z) + \int_0^1 z \, dz P_{VH,G}^R(z) \right], \quad (2.82)$$

from which the Sudakov factor can be constructed using eq. (2.29).

An important aspect of the SU(2) evolution equations is that, contrary to the other gauge groups, the dependence on the ratio m_V/q does not cancel between the real and virtual splitting functions. As an example, consider the evolution equation for an up-type fermion, given on the first line of eq. (2.74), with the virtual contribution given by the first line of eq. (2.80). The sum of the contributions of real and virtual splitting functions is given by

$$\frac{\alpha_2}{\pi} \int_0^{1-\frac{m_V}{q}} dz \frac{1}{4} P_{ff,G}^R(z) [2 f_{d_L}(x/z) + f_{u_L}(x/z) - 3 f_{u_L}(x)] + \dots, \quad (2.83)$$

where \dots represents less singular terms. Thus, the SU(2) breaking in the proton, which renders $f_u(z) \neq f_d(z)$, gives rise to a logarithmic dependence on m_V/q , which leads to a double-logarithmic dependence upon integration over q . As we will see later, the effect of this dependence is to double-logarithmically suppress the SU(2) breaking effects at high energies.

2.8 $I = Y$: Yukawa interactions

The interaction of Higgs particles with fermions is described by the Yukawa interactions. In this work we only keep the top Yukawa coupling, setting all others to zero. This gives the following couplings

$$C_{q_L^3 t_R, Y} = C_{H^0 t_R, Y} = C_{H^+ t_R, Y} = C_{t_R q_L^3, Y} = C_{\bar{H}^0 t_L, Y} = C_{H^- b_L, Y} = 1, \quad (2.84)$$

where q_L^3 denotes either the left-handed top or bottom quark. We furthermore need

$$C_{t^R H^0, Y} = C_{t^R H^+, Y} = C_{t^L \bar{H}^0, Y} = C_{b_L H^-, Y} = N_C. \quad (2.85)$$

This gives contributions to the top quark PDFs, as well as the left-handed bottom PDF:

$$\left[\Delta_{q_L^3, Y} q \frac{\partial}{\partial q} \frac{f_{t_L}}{\Delta_{q_L^3, Y}} \right]_Y = \frac{\alpha_Y}{\pi} \left\{ P_{ff, Y}^R \otimes f_{t_R} + N_C P_{fH, Y} \otimes f_{\bar{H}^0} \right\}, \quad (2.86)$$

$$\left[\Delta_{t_R, Y} q \frac{\partial}{\partial q} \frac{f_{t_R}}{\Delta_{t_R, Y}} \right]_Y = \frac{\alpha_Y}{\pi} \left\{ P_{ff, Y}^R \otimes [f_{t_L} + f_{b_L}] + N_C P_{fH, Y} \otimes [f_{H^0} + f_{H^+}] \right\}, \quad (2.87)$$

$$\left[\Delta_{q_L^3, Y} q \frac{\partial}{\partial q} \frac{f_{b_L}}{\Delta_{q_L^3, Y}} \right]_Y = \frac{\alpha_Y}{\pi} \left\{ P_{ff, Y}^R \otimes f_{t_R} + N_C P_{fH, Y} \otimes f_{H^-} \right\}. \quad (2.88)$$

It also contributes to the evolution of the Higgs bosons:

$$\left[\Delta_{H, Y} q \frac{\partial}{\partial q} \frac{f_{H^+}}{\Delta_{H, Y}} \right]_Y = \frac{\alpha_Y}{\pi} P_{Hf, Y}^R \otimes [f_{t_R} + f_{\bar{b}_L}], \quad (2.89)$$

$$\left[\Delta_{H, Y} q \frac{\partial}{\partial q} \frac{f_{H^0}}{\Delta_{H^0, Y}} \right]_Y = \frac{\alpha_Y}{\pi} P_{Hf, Y}^R \otimes [f_{t_R} + f_{\bar{t}_L}]. \quad (2.90)$$

The Sudakov factors can be obtained using eq. (2.29) with

$$P_{q_L^3, Y}^V(q) = \frac{1}{2} P_{t_R, Y}^V(q) = - \int_0^1 z dz P_{ff, Y}^R(z) - \int_0^1 z dz P_{Hf, Y}^R(z), \quad (2.91)$$

$$P_{H, Y}^V(q) = -2N_C \int_0^1 z dz P_{fH, Y}^R(z). \quad (2.92)$$

2.9 $I = M$: mixed $B - W_3$ interactions

Finally, we need to consider the evolution involving the mixed BW boson PDF. The non-vanishing couplings are

$$C_{BWf_u, M} = -C_{BWf_d, M} = 2 \frac{Y_f}{2}, \quad (2.93)$$

$$C_{f_u BW, M} = -C_{f_d BW, M} = N_f \frac{Y_f}{2}, \quad (2.94)$$

where f_u and f_d represent the up- and down-type left-handed fermions and anti-fermions of all generations. Since $Y_{\bar{f}} = -Y_f$ and $T_{3\bar{f}} = -T_{3f}$, the couplings for fermions and anti-fermions are identical. The factor of 2 in the first line comes from our definition of f_{BW} as the sum of BW and WB contributions. The diagonal coefficients $C_{f_u f_u, M}$ and $C_{f_d f_d, M}$ are zero because there is no vector boson with both U(1) and SU(2) interactions. For the same reason, there are no Sudakov factors associated with the mixed interaction. The couplings involving the Higgs bosons are

$$C_{BWH^+, M} = -C_{BWH^0, M} = \frac{1}{2}, \tag{2.95}$$

$$C_{H^+ BW, M} = -C_{H^0 BW, M} = \frac{1}{4}, \tag{2.96}$$

where, as for the fermions, the same relations hold for the charge-conjugate states.

Plugging these into the general evolution equation gives

$$\left[q \frac{\partial}{\partial q} f_{f_u} \right]_M = \frac{\alpha_M}{\pi} \frac{Y_f}{2} N_f P_{fV, G}^R \otimes f_{BW}, \tag{2.97}$$

$$\left[q \frac{\partial}{\partial q} f_{f_d} \right]_M = -\frac{\alpha_M}{\pi} \frac{Y_f}{2} N_f P_{fV, G}^R \otimes f_{BW}, \tag{2.98}$$

$$\begin{aligned} \left[q \frac{\partial}{\partial q} f_{BW} \right]_M = & \frac{\alpha_M}{\pi} \left[\sum_{f_u} Y_f P_{Vf, G}^R \otimes f_{f_u} - \sum_{f_d} Y_f P_{Vf, G}^R \otimes f_{f_d} \right. \\ & \left. + \frac{1}{2} \sum_{h_u} P_{VH, G}^R \otimes f_{h_u} - \frac{1}{2} \sum_{h_d} P_{VH, G}^R \otimes f_{h_d} \right], \end{aligned} \tag{2.99}$$

$$\left[q \frac{\partial}{\partial q} f_{h_u} \right]_M = \frac{\alpha_M}{\pi} \frac{1}{4} P_{HV, G}^R \otimes f_{BW}, \tag{2.100}$$

$$\left[q \frac{\partial}{\partial q} f_{h_d} \right]_M = -\frac{\alpha_M}{\pi} \frac{1}{4} P_{HV, G}^R \otimes f_{BW}. \tag{2.101}$$

As already discussed, the mixed gauge field PDF f_{BW} has Sudakov factors associated with the U(1) and SU(2) interactions, given by eq. (2.29). Since there is no corresponding real emission term in the evolution equation for f_{BW} , it evolves double-logarithmically and is suppressed at high scales relative to the unmixed PDFs.

3 Implementation details

Our treatment assumes that the SM PDFs at very high energies can be obtained by smoothly matching the broken and unbroken symmetry regimes at a matching scale $q_0 \sim m_V$, which in practice we take to be 100 GeV. Our input PDFs at 100 GeV are obtained as follows. We take the CT14qed PDF set [15] at 10 GeV and replace the photon PDF by that of the LUXqed set [16]. We do not use the CT14qed photon because the LUXqed photon, while being consistent with CT14qed, has much smaller uncertainties and a smoother x dependence. The LUXqed PDF set combines the PDF4LHC15_nnlo_100 parton set [31] with a determination of the photon PDF from structure function and elastic form factor

fits in electron-proton scattering. However, we do not use the LUXqed partons, because being NNLO they are not positive-definite, which we require for our LO treatment and is satisfied by CT14qed.

We evolve this hybrid CT14-LUX PDF set from 10 to 100 GeV using leading-order QCD plus QED evolution, which incidentally generates the charged leptons. The resulting parton, photon and lepton PDFs form our input to the unbroken SM evolution upwards from 100 GeV. The input left- and right-handed fermion PDFs are identical. The input W^3 , B and mixed B/W^3 PDFs are determined by the photon (and the absence of the Z^0) at the matching scale according to eq. (2.7). The remaining vector boson, neutrino and Higgs PDFs are all generated dynamically starting from zero at the matching scale.

The equations given in sections 2.5 to 2.9 completely define the evolution of all parton distribution functions in the unbroken symmetry regime. However, as already explained, one can rewrite the equations slightly to make them more amenable to a numerical implementation. First, switching to a basis of states with well-defined isospin decouples the set of 52 equations to some degree. In this new basis another transformation eliminates the double logarithmic sensitivity to the ratio m_V/q . Second, by combining the virtual and real splitting functions into +-distributions, one can reduce numerical sensitivity to the cutoff of the z integrations. We will now discuss these simplifications in turn.

3.1 Switching to a basis of conserved quantum numbers

As we already explained in section 2.2, the set of 52 evolution equations can be decoupled to some degree by switching to a basis of well-defined isospin \mathbf{T} and CP. Writing a fermion PDF with \mathbf{T} and CP as $f_i^{\mathbf{T}CP}$, we write the left-handed fermions as

$$f_{f_L}^{0+} = \frac{1}{4} (f_{u_L} + f_{d_L} + f_{\bar{d}_L} + f_{\bar{u}_L}) , \quad f_{f_L}^{1+} = \frac{1}{4} (f_{u_L} - f_{d_L} - f_{\bar{d}_L} + f_{\bar{u}_L}) , \quad (3.1)$$

$$f_{f_L}^{0-} = \frac{1}{4} (f_{u_L} + f_{d_L} - f_{\bar{d}_L} - f_{\bar{u}_L}) , \quad f_{f_L}^{1-} = \frac{1}{4} (f_{u_L} - f_{d_L} + f_{\bar{d}_L} - f_{\bar{u}_L}) , \quad (3.2)$$

where u_L and d_L refer to left-handed up- and down-type fermions. Right-handed fermions are given by

$$f_{f_R}^{0+} = \frac{1}{2} (f_{f_R} + f_{\bar{f}_R}) , \quad f_{f_R}^{0-} = \frac{1}{2} (f_{f_R} - f_{\bar{f}_R}) . \quad (3.3)$$

The SU(3) and U(1) boson PDFs have $\mathbf{T} = 0$, CP = +

$$f_g^{0+} = f_g , \quad f_B^{0+} = f_B , \quad (3.4)$$

while the SU(2) boson PDFs can have $\mathbf{T} = 0, 1, 2$ with respectively CP = +, -, +

$$f_W^{0+} = \frac{1}{3} (f_{W^+} + f_{W^-} + f_{W^0}) , \quad f_W^{1-} = \frac{1}{2} (f_{W^+} - f_{W^-}) , \quad (3.5)$$

$$f_W^{2+} = \frac{1}{6} (f_{W^+} + f_{W^-} - 2f_{W^0}) . \quad (3.6)$$

The mixed BW boson state is a combination of 0^- and 1^- and therefore its PDF has $\mathbf{T} = 1$, CP = +

$$f_{BW}^{1+} = f_{BW} . \quad (3.7)$$

For the Higgs boson, one writes similarly to the fermions

$$f_H^{0+} = \frac{1}{4}(f_{H^+} + f_{H^0} + f_{\bar{H}^0} + f_{H^-}), \quad f_H^{1+} = \frac{1}{4}(f_{H^+} - f_{H^0} - f_{\bar{H}^0} + f_{H^-}), \quad (3.8)$$

$$f_H^{0-} = \frac{1}{4}(f_{H^+} + f_{H^0} - f_{\bar{H}^0} - f_{H^-}), \quad f_H^{1-} = \frac{1}{4}(f_{H^+} - f_{H^0} + f_{\bar{H}^0} - f_{H^-}). \quad (3.9)$$

In terms of these states the longitudinal vector boson and Higgs PDFs are then, using eq. (2.16),

$$f_{W_L^+} = f_H^{0+} + f_H^{1+} + f_H^{0-} + f_H^{1-}, \quad (3.10)$$

$$f_{W_L^-} = f_H^{0+} + f_H^{1+} - f_H^{0-} - f_H^{1-}, \quad (3.11)$$

$$f_{Z_L} = f_h = f_H^{0+} - f_H^{1+}. \quad (3.12)$$

3.2 Cancellation of double-logarithmic dependence in evolution equations

In the $\{\mathbf{T}, \text{CP}\}$ basis the singular contributions to the evolution equations (those that are proportional to the splitting functions $P_{ff,G}^R(z)$, $P_{VV,G}^R(z)$ and $P_{HH,G}^R(z)$, which diverge in the limit $z \rightarrow 1$) are diagonal,

$$\left[\Delta_{i,I} q \frac{\partial}{\partial q} \frac{f_i^{\text{TCP}}}{\Delta_{i,I}} \right]_I = \frac{\alpha_I}{\pi} D_{i,I}^{\text{TCP}} P_{ii,I}^R \otimes f_i^{\text{TCP}} + \dots, \quad (3.13)$$

such that the PDF multiplying the divergent splitting function is the same as that appearing on the left-hand side. Here, as in f_i^{TCP} , the label i now refers to a parton species f, V, H rather than a particular parton. Recalling that the Sudakov factor takes the form

$$\begin{aligned} \Delta_{i,I}(q) &= \exp \left[\int_{q_0}^q \frac{dq'}{q'} \frac{\alpha_I(q')}{\pi} P_{i,I}^V(q') \right] \\ &= \exp \left[-C_{i,I} \int_{q_0}^q \frac{dq'}{q'} \frac{\alpha_I(q')}{\pi} \int_0^{z_{\max}^{ii,I}(q)} z dz P_{ii,I}^R(z) + \dots \right], \end{aligned} \quad (3.14)$$

where \dots represents less divergent terms, and

$$C_{i,I} = \sum_{k \in i} C_{kl,I} \text{ for } l \in i, \quad (3.15)$$

where k and l are particular partons, we have

$$\begin{aligned} \left[q \frac{\partial}{\partial q} f_i^{\text{TCP}} \right]_I &= \frac{\alpha_I}{\pi} \left[D_{i,I}^{\text{TCP}} P_{ii,I}^R \otimes f_i^{\text{TCP}} + P_{i,I}^V f_i^{\text{TCP}} \right] + \dots, \\ &= \frac{\alpha_I}{\pi} \left[D_{i,I}^{\text{TCP}} P_{ii,I}^+ \otimes f_i^{\text{TCP}} + \left(1 - \frac{D_{i,I}^{\text{TCP}}}{C_{i,I}} \right) P_{i,I}^V f_i^{\text{TCP}} \right] + \dots, \end{aligned} \quad (3.16)$$

where

$$\begin{aligned} P_{ii,I}^+ \otimes f_i &\equiv P_{ii,I}^R \otimes f_i + \frac{P_{i,I}^V}{C_{i,I}} f_i \\ &= \int_0^{z_{\max}^{ii,I}(q)} dz \left[P_{ii,I}^R(z) \theta(z > x) f(x/z, q) - z P_{ii,I}^R(z) f(x, q) \right] + \dots \end{aligned} \quad (3.17)$$

The +-prescription defined by eq. (3.17) regulates the divergence in the integrand as $z \rightarrow 1$ and therefore if we define the modifying factor

$$\begin{aligned} F_{i,I}^{\text{TCP}}(q) &= \exp \left[\left(1 - \frac{D_{i,I}^{\text{TCP}}}{C_{i,I}} \right) \int_{q_0}^q \frac{dq'}{q'} \frac{\alpha_I(q')}{\pi} P_{i,I}^V(q') \right] \\ &= [\Delta_{i,I}(q)]^{1-D_{i,I}^{\text{TCP}}/C_{i,I}}, \end{aligned} \quad (3.18)$$

then the evolution equation (3.13) becomes

$$\left[F_{i,I}^{\text{TCP}} q \frac{\partial}{\partial q} \frac{f_i^{\text{TCP}}}{F_{i,I}^{\text{TCP}}} \right]_I = \frac{\alpha_I}{\pi} D_{i,I}^{\text{TCP}} P_{ii,I}^+ \otimes f_i^{\text{TCP}} + \dots, \quad (3.19)$$

with no logarithmic dependence on m_V/q on the right-hand side.

For all interactions except SU(2), one can show that $D_{i,I}^{\text{TCP}} = C_{i,I}$, so that the modifying factor (3.18) is unity.⁷ For SU(2) we have explicitly:⁸

$$C_{f,2} = C_{H,2} = \frac{3}{4}, \quad C_{V,2} = 2, \quad (3.20)$$

while

$$D_{f,2}^{0\pm} = D_{H,2}^{0\pm} = \frac{3}{4}, \quad D_{f,2}^{1\pm} = D_{H,2}^{1\pm} = -\frac{1}{4}, \quad (3.21)$$

$$D_{V,2}^{0+} = 2, \quad D_{V,2}^{1-} = 1, \quad D_{V,2}^{2+} = -1, \quad (3.22)$$

so that

$$F_{f,2}^{0\pm} = F_{H,2}^{0\pm} = 1, \quad F_{f/H,2}^{1\pm} = \Delta_{f/H,2}^{4/3}, \quad (3.23)$$

$$F_{V,2}^{0+} = 1, \quad F_{V,2}^{1-} = \Delta_{V,2}^{1/2}, \quad F_{V,2}^{2+} = \Delta_{V,2}^{3/2}. \quad (3.24)$$

For the mixed PDF f_{BW} we have $D_{BW,2}^{1+} = 0$ and therefore

$$F_{BW,2}^{1+} = \Delta_{BW,2} = \Delta_{V,2}^{1/2} = F_{V,2}^{1-} \quad (3.25)$$

The equations finally used to evolve the PDFs in the conserved-quantum-number basis are given in appendix A.

4 Results

We begin by showing how the PDFs of strongly interacting particles are changed by including the evolution of the full Standard Model. Figure 1 shows results on the evolution of left- and right-handed quark PDFs, shown solid and dashed respectively, normalized to their values assuming pure QCD evolution. In each plot we show the results at three different scales, namely $q = 10^4$ GeV, $q = 10^6$ GeV and $q = 10^8$ GeV. The values of 10^6 and 10^8 GeV are of course far away from energy scales one can reach at any collider in the near or distant future. However, showing the results at such unattainable values helps to illustrate their approach to asymptotic behavior.

⁷For the U(1) interaction one has $D_{i,1}^{\text{TCP}} = C_{i,1} = 0$, and we choose to set the modifying factor to 1 in this case.

⁸Here we have used the numerical values for the Casimir operator eigenvalues for the corresponding SU(2) representations, $C_F^{\text{SU}(2)} = 3/4$, $C_A^{\text{SU}(2)} = 2$.

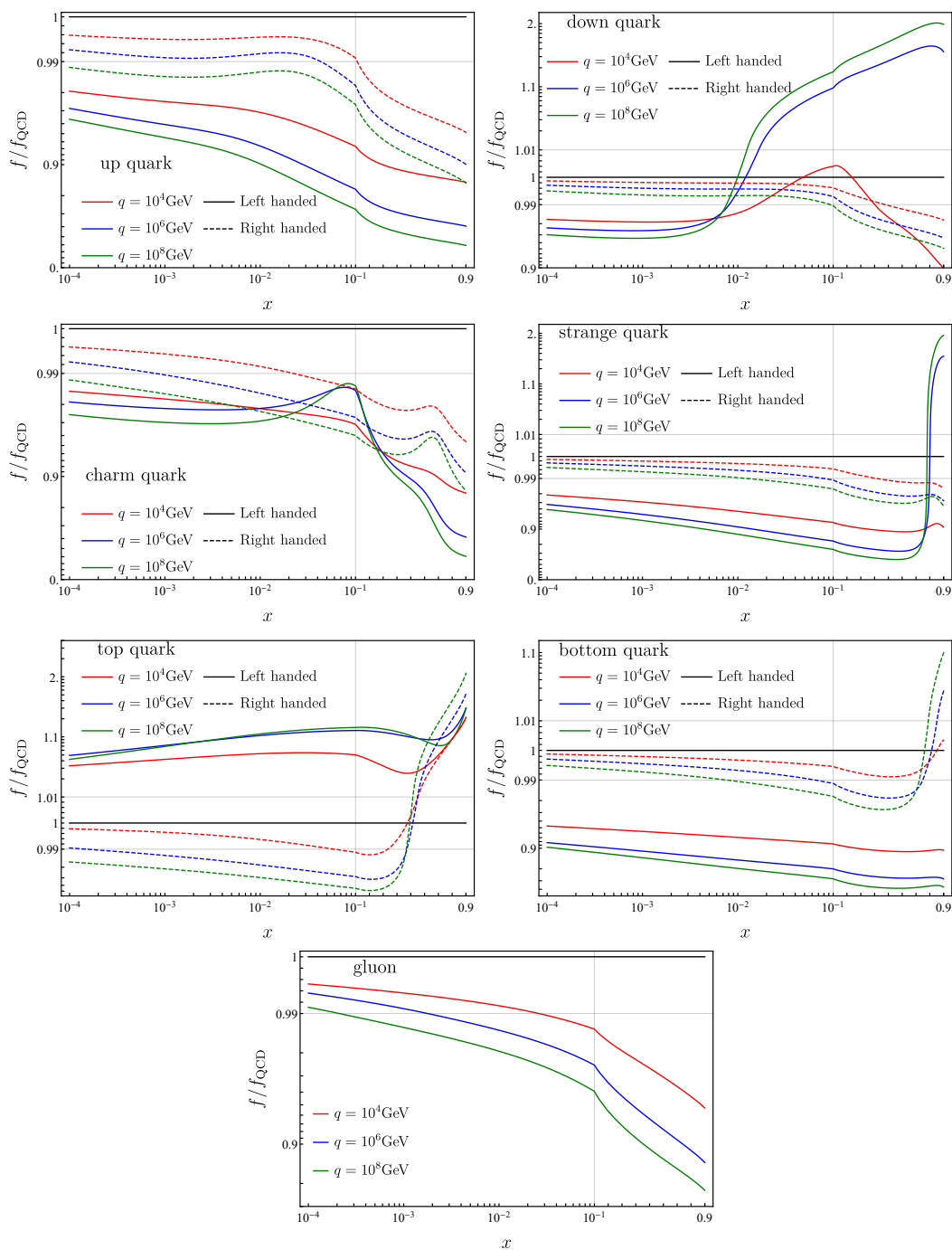


Figure 1. Quark and gluon PDFs in the full unbroken SM, divided by their values assuming pure QCD evolution only. Left- and right-handed quark chiralities are solid and dashed, respectively. The thin gray lines show where the scales on the x- and/or y-axes switch between linear and logarithmic.

All the light quarks (and antiquarks, not shown) evolve to lower values compared to pure QCD at small x , due to an overall loss of energy to the electroweak gauge bosons through the additional splittings $q \rightarrow qW$ and $q \rightarrow qB$. At higher x values, the up and

down quarks (top row) exhibit different behaviors, with the left-handed up PDF evolving more rapidly to lower values compared to pure QCD, while the down quark eventually evolves to higher values. This is because the left-handed up and down distributions evolve towards each other, their difference being double-logarithmically suppressed at high scales. The right-handed quark PDFs have no double-logarithmic component and evolve to slightly lower values than pure QCD, due to energy loss through the additional splitting $q_R \rightarrow q_R B$.

The asymmetry between left-handed charm and strange quarks also evolves double-logarithmically towards zero, primarily through a more rapid decrease of the strange PDF. At high x the behavior is more complicated because the input CT14qed charm PDF is larger than the strange above $x \sim 0.7$. The right-handed quarks behave qualitatively the same as those of the first generation.

The left-handed top and bottom quarks also must evolve towards equal values, which in this case means that the top has higher values than in pure QCD, while the bottom evolution looks similar to strange, relative to pure QCD. The right-handed b -quark behaves qualitatively like the right-handed quarks of the first and second generation, while the right-handed top quark, being generated purely dynamically, behaves differently at large x . Since the right-handed top has vanishing initial condition, the splitting $t_R \rightarrow t_R B$, which would decrease the PDF, is sub-dominant compared to the process $B \rightarrow t_R \bar{t}_R$. This means that at large x the right-handed top PDF is increased, rather than decreased.

The effect on the gluon PDF is shown in last row of figure 1. While the effects are quite small up to $q \sim 10^4$ GeV, at larger scales the back-reaction from the changing quark PDFs is affecting the gluon PDF at an appreciable level.

It is interesting to study how rapidly electroweak symmetry is restored. To illustrate this, we show the asymmetry

$$A^{qL} = \frac{f_{uL} - f_{dL}}{f_{uL} + f_{dL}}, \tag{4.1}$$

compared to the result if only QCD evolution were turned on. This asymmetry ratio is shown in figure 2 for the three generation of quarks as a function of q , for various values of x . For all generations the asymmetry decreases as q gets larger, driving the PDFs of the different isospin states towards each other. The onset of the deviation from pure QCD is in the range 1–10 TeV. The ratio between the full asymmetry and the result using only QCD evolution is given by

$$A^{qL}(x, q) \sim [\Delta_{f,2}(q)]^{4/3} A_{\text{QCD}}^{qL}(x, q) \tag{4.2}$$

where $\Delta_{f,2}(q)$ is the fermion Sudakov factor, as given in eq. (3.18), independent of the generation.

Next, we study the size of the PDFs of particles not charged under the strong interaction. Since these PDFs are only generated by emissions due to the U(1), SU(2) or Yukawa interactions, they are vanishing at all scales if one is including only SU(3) evolution. The only exception is the photon, which has a non-vanishing initial condition at $q = 100$ GeV. Figure 3 shows results on the electroweak boson PDFs normalized to the gluon PDF, both evolved using the full Standard Model. One can see that the electroweak gauge boson PDFs become a significant fraction of the gluon PDF, especially at large values of x . The photon PDF is the largest mainly because it has a non-zero input. The PDF for the W^+

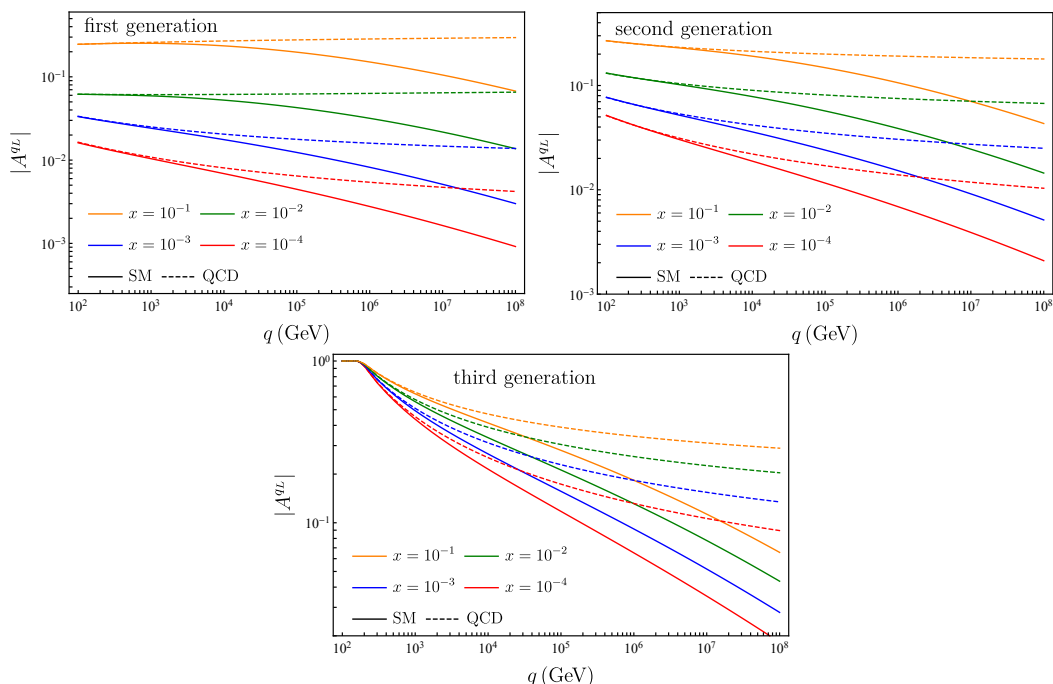


Figure 2. Asymmetry between up-isospin and down-isospin left-handed quark PDFs, defined in eq. (4.1), in the full unbroken SM, compared to the result when only QCD evolution is included.

boson is initially larger than the W^- boson PDF at large x because the W^+ is mainly generated through emissions from the up-quark, whose PDF is larger than the down-quark which mainly generates the W^- . Since the difference between W^+ and W^- has isospin 1, the W^+ evolves more slowly and the W^- more rapidly, so that they approach each other at high q . At low x they are more similar as are the up-quark and down-quark PDFs. The Z^0 PDF is similar to the W^+ but it is smaller at low x and larger at large x . The mixed γZ PDF is small and positive at small x and negative at large x . There is no constraint to be positive definite for a mixed PDF as it is the product of two amplitudes rather than the square modulus of one. Its absolute value becomes very large at large x and q .

We also show the PDFs for the longitudinally polarized gauge bosons, the Higgs boson, the mixed PDF between the Higgs and the Z_L and the leptons. The Z_L PDF is the same as the Higgs in our approximation, see eq. (2.16), so we do not make a separate plot for it. The boson PDFs are shown in figure 4, and the leptons in figure 5, both normalized to the gluon. Both are expected to be much smaller than the transverse vector boson PDFs, because they are generated via a second order effect of emission from the vector bosons and via Yukawa emission from the top and bottom quarks, which are much smaller than the up and down quarks. The mixed PDF is even smaller because it is generated by the asymmetry between transverse W^+ and W^- PDFs and the top and anti-top PDFs. The W_L^+ and W_L^- PDFs are very similar, for the same reason.

As a final result, we study several parton luminosities, choosing a future 100 TeV pp collider as a reference. While the energy scales that can be reached at such a collider

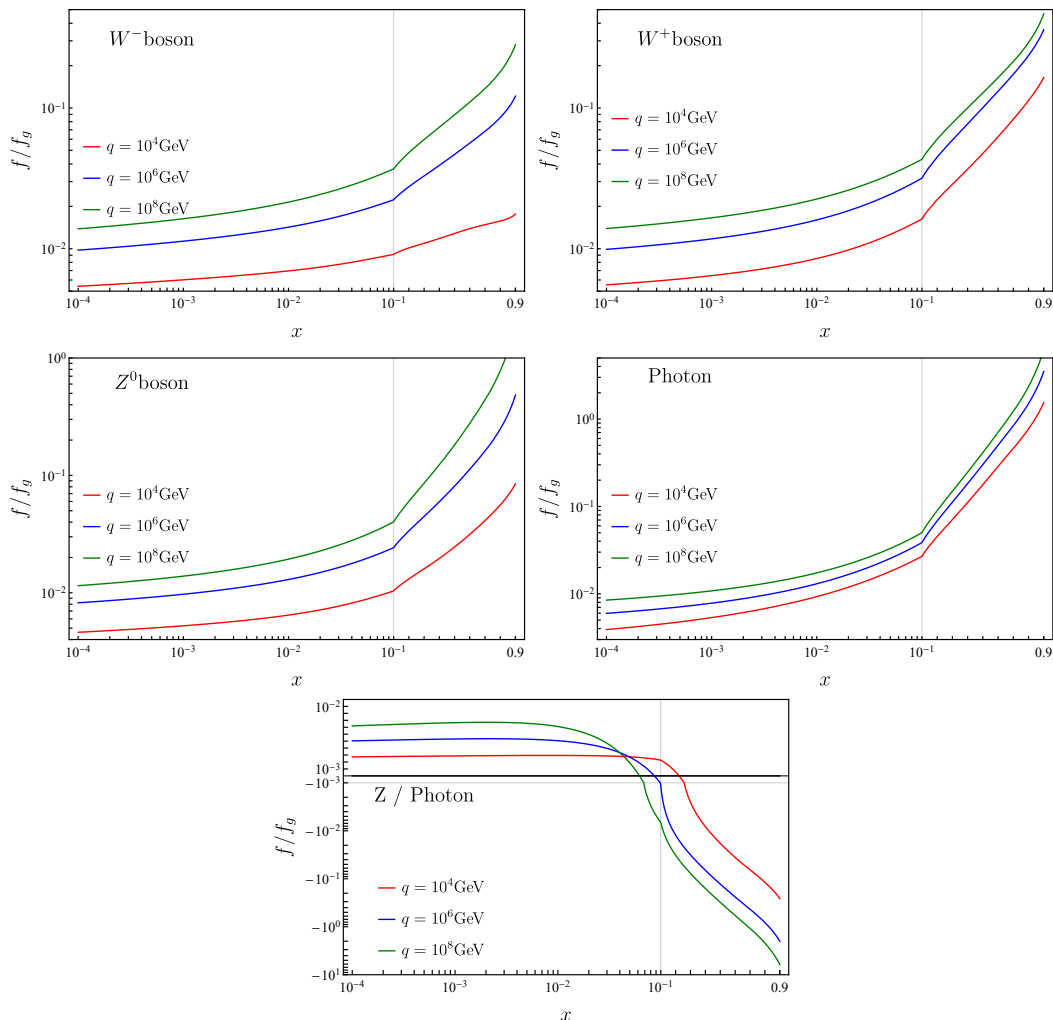


Figure 3. Electroweak bosons PDF normalized by the gluon PDF. The thin gray lines show where the scales on the x- and/or y-axes switch between linear and logarithmic.

are not quite large enough to get $\mathcal{O}(1)$ effects, the effects of the full Standard Model evolution are still numerically relevant. In figure 6 we show the $q_L \bar{q}_L$ luminosities for the six different quark flavors, normalized to their values if only QCD evolution is taken into account. One can see that all except the $t\bar{t}$ luminosity are reduced appreciably from their values if only QCD evolution were taken into account. This will affect searches for Z' -like particles at a future 100 TeV collider. The $d\bar{d}$ luminosity is decreasing more slowly as the double-logarithmic evolution drives it larger than QCD at high x (see figure 1).

We also show selected luminosities of vector bosons combined with quarks, normalized to the average of the $u\bar{u}$ and $d\bar{d}$ luminosities. One can see that luminosities involving one transverse vector boson become of comparable magnitude to the $q\bar{q}$ luminosities. Luminosities involving the longitudinal gauge and Higgs bosons are much smaller.

Finally, to illustrate the uncertainties associated with subleading terms, we show in tables 2 and 3 the dependence of some integrated PDFs (momentum fractions) on the in-

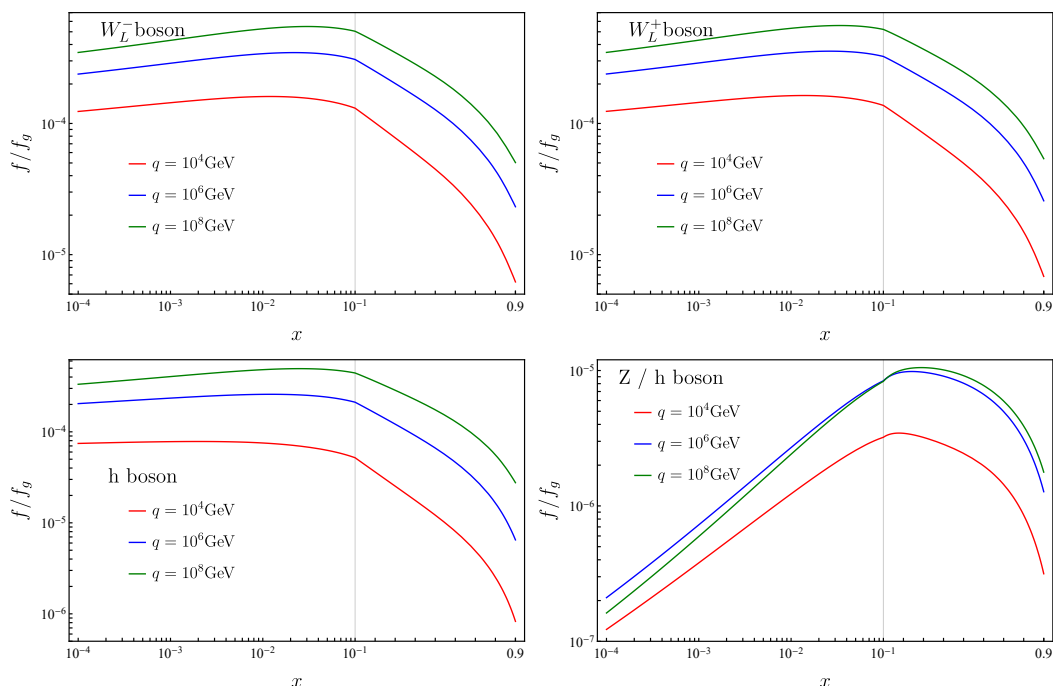


Figure 4. Longitudinal gauge and Higgs bosons PDFs normalized by the gluon PDF. The Z_L PDF is the same as the h PDF. The hZ_L PDF is purely imaginary and we show the result divided by i . The thin gray line shows where the scales on the x- and/or y-axes switch between linear and logarithmic.

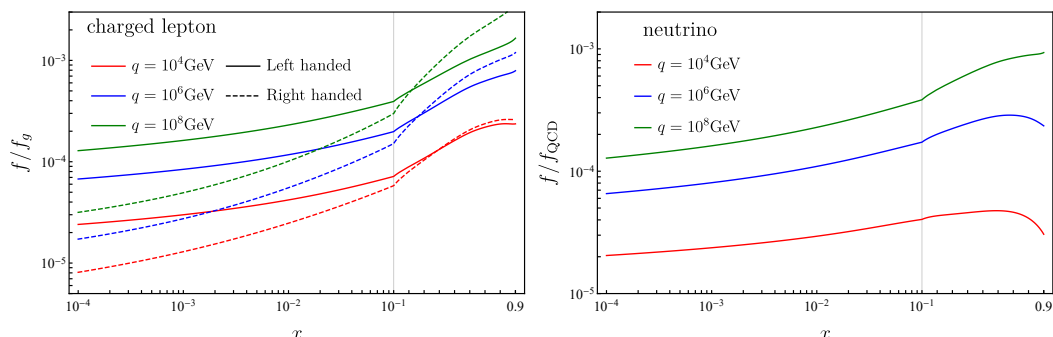


Figure 5. First generation lepton PDFs normalized by the gluon PDF. Since we treat leptons as massless, and all leptons have the same initial condition, the results for the other 2 generations are identical. The thin gray line shows where the scales on the x- and/or y-axes switch between linear and logarithmic.

frared cutoff m_V and matching scale q_0 . We see that there are variations in the electroweak PDFs of the order of $\pm 10\%$ at 10 TeV and 5% at 100 TeV for the ranges of parameters indicated. The relative variations in the light quark PDFs are smaller as they are dominated by QCD evolution. There are of course in addition the usual uncertainties associated with the input PDFs and higher-order QCD corrections.

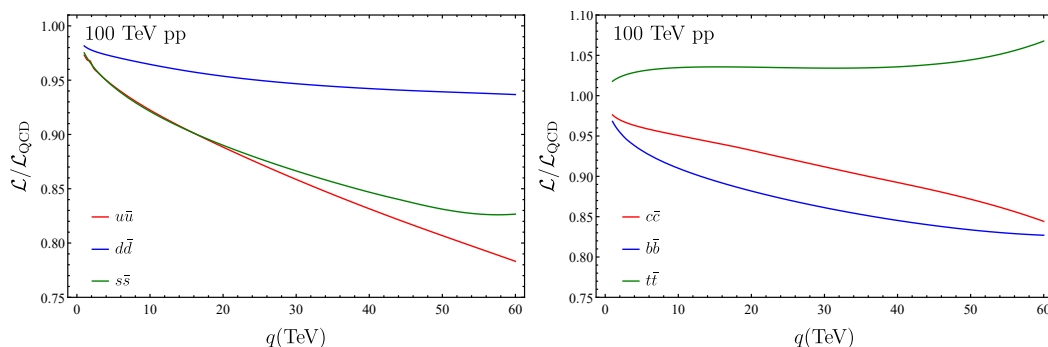


Figure 6. Quark anti-quark luminosity in the full unbroken SM, divided by their values assuming pure QCD evolution only.

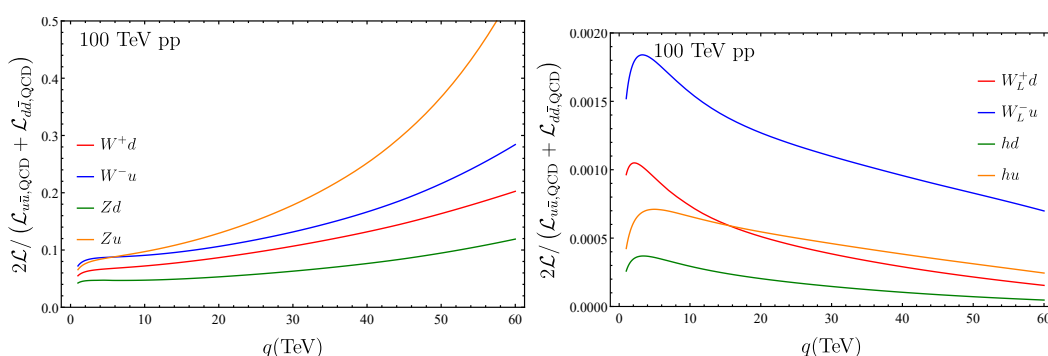


Figure 7. Vq and Hq luminosity in the full unbroken SM, divided by the average of $u\bar{u}$ and $d\bar{d}$ luminosity assuming pure QCD evolution only.

m_V/GeV	q_0/GeV	u_L	t_L	W_T^+	W_T^-	e_L^-	ν_e	h
100	100	8.51	0.43	0.46	0.33	0.0019	0.0012	0.0026
50	100	8.42	0.43	0.46	0.34	0.0019	0.0012	0.0027
50	200	8.48	0.44	0.39	0.29	0.0017	0.0009	0.0025
100	200	8.56	0.43	0.39	0.29	0.0017	0.0009	0.0024
200	200	8.64	0.42	0.39	0.28	0.0017	0.0009	0.0024

Table 2. Momentum fractions (%) carried by various parton species at scale $q = 10$ TeV.

m_V/GeV	q_0/GeV	u_L	t_L	W_T^+	W_T^-	e_L^-	ν_e	h
100	100	7.53	0.56	0.64	0.50	0.0031	0.0025	0.0061
50	100	7.43	0.61	0.63	0.51	0.0031	0.0026	0.0062
50	200	7.48	0.61	0.58	0.47	0.0028	0.0021	0.0059
100	200	7.58	0.60	0.58	0.46	0.0028	0.0021	0.0055
200	200	7.68	0.59	0.58	0.45	0.0028	0.0020	0.0054

Table 3. Momentum fractions (%) carried by various parton species at scale $q = 100$ TeV.

5 Conclusions

The energy regime around and beyond the electroweak scale is currently being explored by the LHC experiments, and so far they have found no firm evidence for physics beyond the Standard Model. In the present paper, we have examined the consequences of assuming that the parton distributions of the proton continue to be described by the Standard Model up to very high energies, in the approximation that its symmetries are unbroken above the electroweak scale.

We have implemented numerically the full set of generalized DGLAP evolution equations for all the parton species and interactions of the unbroken SM in leading order. The input PDFs of 5 quark flavors, the gluon, photon and charged leptons at a starting scale $q_0 = 100 \text{ GeV}$ for the full SM evolution are obtained from parton and photon PDFs at 10 GeV by QCD plus QED evolution. The input left- and right-handed fermion PDFs are thus identical at scale q_0 but they evolve differently above that scale. The top quark PDFs (not present in the input) start to evolve from the top mass scale. The input photon is resolved into its U(1), SU(2) and mixed components, which are evolved independently from scale q_0 and reassembled into the photon and transversely polarized Z^0 at higher scales. The charged and longitudinal vector boson, Higgs and neutrino PDFs are generated dynamically starting from zero at scale q_0 . This simplified treatment misses some symmetry-breaking effects around the electroweak scale, but these are power-suppressed at higher scales and our results should provide a guide to the ways in which the PDFs deviate from pure QCD evolution.

Amongst the most interesting features of the SM is the distinction between left- and right-handed fermions. The evolution of the right-handed PDFs deviates little from pure QCD, owing to the weakness of the U(1) interaction. The left-handed PDFs generally deviate from pure QCD at the 5–10% level by 10 TeV .

Another important SM characteristic is the restoration of isospin symmetry at high scales. This is manifest in the decreasing asymmetry between the up- and down-type quark PDFs, which sets in at $1\text{--}10 \text{ TeV}$, the up-type being pulled down in the first generation and conversely in the third. The suppression of the asymmetry is a double-logarithmic effect that can be treated in fixed order at present energies but is resummed to all orders in the evolution.

The electroweak bosons are generated quite copiously, the W^+ in particular at high x due to splitting $u \rightarrow dW^+$. The photon and Z^0 PDFs also grow rapidly, eventually exceeding the gluon at high x . The PDFs of the longitudinal vector bosons, the Higgs boson and the leptons are generally much smaller as they arise from second-order splittings.

Finally, we have used the generated PDFs to present some parton-parton luminosities at a 100 TeV pp collider. These results are just an illustration of the size of the effects that can be expected at such a future collider, and a more detailed phenomenological analysis will be presented in a forthcoming publication.

In conclusion, we find a rich structure in the proton when probed beyond the electroweak scale. The associated PDFs are interesting and useful in their own right. They also represent a key component of event generators that aim to embody the full Standard Model in initial-state parton showering, a topic we plan to explore further.

Acknowledgments

We thank Gavin Salam and Denis Comelli for comments on the manuscript. This work was supported by the Director, Office of Science, Office of High Energy Physics of the U.S. Department of Energy under the Contract No. DE-AC02-05CH11231 (CWB, NF), and partially supported by STFC consolidated grant ST/L000385/1 (BRW).

A Equations used in the forward evolution

A.1 SU(3) interaction

- $\mathbf{T} = 0$ and $\text{CP} = +$:

$$\left[q \frac{\partial}{\partial q} f_q^{0+} \right]_3 = \frac{\alpha_3}{\pi} \left[C_F P_{ff,G}^+ \otimes f_q^{0+} + T_R P_{fV,G}^R \otimes f_g \right], \quad (\text{A.1})$$

$$\left[q \frac{\partial}{\partial q} f_g \right]_3 = \frac{\alpha_3}{\pi} \left[C_A P_{VV,G}^+ \otimes f_g + C_F P_{Vf,G}^R \otimes f_{\Sigma_g}^{0+} \right]. \quad (\text{A.2})$$

Here

$$f_{\Sigma_g}^{0+} = 4 \sum_{q_L} f_{q_L}^{0+} + 2 \sum_{q_R} f_{q_R}^{0+}, \quad (\text{A.3})$$

where the sums run over all left-handed quark doublets and all right-handed quarks. The factors of 4 and 2 are due to the different normalizations in eqs. (3.1) and (3.3).

- All other states:

$$\left[q \frac{\partial}{\partial q} f_q \right]_3 = \frac{\alpha_3}{\pi} C_F P_{ff,G}^+ \otimes f_q. \quad (\text{A.4})$$

A.2 U(1) interaction

- $\mathbf{T} = 0$ and $\text{CP} = +$:

$$\left[q \frac{\partial}{\partial q} f_f^{0+} \right]_1 = \frac{\alpha_1}{\pi} Y_i^2 \left[P_{ff,G}^+ \otimes f_f^{0+} + N_f P_{fV,G}^R \otimes f_B \right], \quad (\text{A.5})$$

$$\left[q \frac{\partial}{\partial q} f_B \right]_1 = \frac{\alpha_1}{\pi} \left[P_{B,1}^V f_B + P_{Vf,G}^R \otimes f_{\Sigma_B}^{0+} + P_{VH,G}^R \otimes f_H^{0+} \right], \quad (\text{A.6})$$

$$\left[q \frac{\partial}{\partial q} f_H^{0+} \right]_1 = \frac{\alpha_1}{\pi} \frac{1}{4} \left[P_{HH,G}^+ \otimes f_H^{0+} + P_{HV,G}^R \otimes f_B \right], \quad (\text{A.7})$$

where

$$f_{\Sigma_B}^{0+} = 4 \sum_{f_L} Y_{f_L}^2 f_{f_L}^{0+} + 2 \sum_{f_R} Y_{f_R}^2 f_{f_R}^{0+}. \quad (\text{A.8})$$

- $\mathbf{T} = 1$ and $\text{CP} = +$:

$$\left[q \frac{\partial}{\partial q} f_{BW}^{1+} \right]_1 = \frac{\alpha_1}{\pi} \frac{1}{2} P_{B,1}^V f_{BW}^{1+}. \quad (\text{A.9})$$

- All other states:

$$\left[q \frac{\partial}{\partial q} f_f \right]_1 = \frac{\alpha_1}{\pi} Y_f^2 P_{ff,G}^+ \otimes f_f, \quad (\text{A.10})$$

$$\left[q \frac{\partial}{\partial q} f_H \right]_1 = \frac{\alpha_1}{\pi} \frac{1}{4} P_{HH,G}^+ \otimes f_H. \quad (\text{A.11})$$

A.3 SU(2) interaction

- $\mathbf{T} = 0$ and $\text{CP} = +$:

$$\left[q \frac{\partial}{\partial q} f_{f_L}^{0+} \right]_2 = \frac{\alpha_2}{\pi} \frac{3}{4} \left[P_{ff,G}^+ \otimes f_{f_L}^{0+} + N_f P_{fV,G}^R \otimes f_W^{0+} \right], \quad (\text{A.12})$$

$$\left[q \frac{\partial}{\partial q} f_W^{0+} \right]_2 = \frac{\alpha_2}{\pi} \left[2P_{VV,G}^+ \otimes f_W^{0+} + \sum_{f_L} P_{Vf,G}^R \otimes f_{f_L}^{0+} + P_{VH,G}^R \otimes f_H^{0+} \right], \quad (\text{A.13})$$

$$\left[q \frac{\partial}{\partial q} f_H^{0+} \right]_2 = \frac{\alpha_2}{\pi} \frac{3}{4} \left[P_{HH,G}^+ \otimes f_H^{0+} + P_{HV,G}^R \otimes f_W^{0+} \right]. \quad (\text{A.14})$$

- $\mathbf{T} = 0$ and $\text{CP} = -$:

$$\left[q \frac{\partial}{\partial q} f_{f_L}^{0-} \right]_2 = \frac{\alpha_2}{\pi} \frac{3}{4} P_{ff,G}^+ \otimes f_{f_L}^{0-}, \quad (\text{A.15})$$

$$\left[q \frac{\partial}{\partial q} f_H^{0-} \right]_2 = \frac{\alpha_2}{\pi} \frac{3}{4} P_{HH,G}^+ \otimes f_H^{0-}. \quad (\text{A.16})$$

- $\mathbf{T} = 1$ and $\text{CP} = +$:

$$\left[\Delta_{f,2}^{4/3} q \frac{\partial}{\partial q} \frac{f_{f_L}^{1+}}{\Delta_{f,2}^{4/3}} \right]_2 = -\frac{\alpha_2}{\pi} \frac{1}{4} P_{ff,G}^+ \otimes f_{f_L}^{1+} \quad (\text{A.17})$$

$$\left[\Delta_{H,2}^{4/3} q \frac{\partial}{\partial q} \frac{f_H^{1+}}{\Delta_{H,2}^{4/3}} \right]_2 = -\frac{\alpha_2}{\pi} \frac{1}{4} P_{HH,G}^+ \otimes f_H^{1+} \quad (\text{A.18})$$

$$\left[\Delta_{V,2}^{1/2} q \frac{\partial}{\partial q} \frac{f_{BW}^{1+}}{\Delta_{V,2}^{1/2}} \right]_2 = 0. \quad (\text{A.19})$$

- $\mathbf{T} = 1$ and $\text{CP} = -$:

$$\left[\Delta_{f,2}^{4/3} q \frac{\partial}{\partial q} \frac{f_{f_L}^{1-}}{\Delta_{f,2}^{4/3}} \right]_2 = \frac{\alpha_2}{\pi} \left[-\frac{1}{4} P_{ff,G}^+ \otimes f_{f_L}^{1-} + \frac{1}{2} N_f P_{fV,G}^R \otimes f_W^{1-} \right] \quad (\text{A.20})$$

$$\left[\Delta_{V,2}^{1/2} q \frac{\partial}{\partial q} \frac{f_W^{1-}}{\Delta_{V,2}^{1/2}} \right]_2 = \frac{\alpha_2}{\pi} \left[P_{VV,G}^+ \otimes f_W^{1-} + \sum_{f_L} P_{Vf} \otimes f_{f_L}^{1-} + P_{VH} \otimes f_H^{1-} \right] \quad (\text{A.21})$$

$$\left[\Delta_{H,2}^{4/3} q \frac{\partial}{\partial q} \frac{f_H^{1-}}{\Delta_{H,2}^{4/3}} \right]_2 = \frac{\alpha_2}{\pi} \left[-\frac{1}{4} P_{HH,G}^+ \otimes f_H^{1-} + \frac{1}{2} P_{HV,G} \otimes f_W^{1-} \right]. \quad (\text{A.22})$$

- $\mathbf{T} = 2$ and $\text{CP} = +$:

$$\left[\Delta_{V,2}^{3/2} q \frac{\partial}{\partial q} \frac{f_W^{2+}}{\Delta_{V,2}^{3/2}} \right]_2 = -\frac{\alpha_2}{\pi} P_{VV}^+ \otimes f_W^{2+}. \quad (\text{A.23})$$

A.4 Yukawa interaction

- $\mathbf{T} = 0$ and $\text{CP} = +$:

$$\left[q \frac{\partial}{\partial q} f_{q_L^3}^{0+} \right]_Y = \frac{\alpha_Y}{\pi} \left[P_{q_L^3, Y}^V f_{q_L^3}^{0+} + P_{ff, Y}^R \otimes f_{t_R}^{0+} + N_c P_{fH, Y} \otimes f_H^{0+} \right] \quad (\text{A.24})$$

$$\left[q \frac{\partial}{\partial q} f_{t_R}^{0+} \right]_Y = \frac{\alpha_Y}{\pi} 2 \left[P_{t_R, Y}^V f_{t_R}^{0+} + P_{ff, Y}^R \otimes f_{q_L^3}^{0+} + N_c P_{fH, Y} \otimes f_H^{0+} \right] \quad (\text{A.25})$$

$$\left[q \frac{\partial}{\partial q} f_H^{0+} \right]_Y = \frac{\alpha_Y}{\pi} \left[P_{H, Y}^V f_H^{0+} + P_{Hf, Y}^R \otimes f_{\sum_H f}^{0+} \right], \quad (\text{A.26})$$

where

$$f_{\sum_H f}^{0+} = f_{t_R}^{0+} + f_{q_L^3}^{0+}. \quad (\text{A.27})$$

- $\mathbf{T} = 0$ and $\text{CP} = -$:

$$\left[q \frac{\partial}{\partial q} f_{q^3}^{0-} \right]_Y = \frac{\alpha_Y}{\pi} \left[P_{q_L^3, Y}^V f_{q_L^3}^{0-} + P_{ff, Y}^R \otimes f_{t_R}^{0-} - N_c P_{fH, Y} \otimes f_H^{0-} \right] \quad (\text{A.28})$$

$$\left[q \frac{\partial}{\partial q} f_{t_R}^{0-} \right]_Y = \frac{\alpha_Y}{\pi} 2 \left[P_{t_R, Y}^V f_{t_R}^{0-} + P_{ff, Y}^R \otimes f_{q^3}^{0-} + N_c P_{fH, Y} \otimes f_H^{0-} \right] \quad (\text{A.29})$$

$$\left[q \frac{\partial}{\partial q} f_H^{0-} \right]_Y = \frac{\alpha_Y}{\pi} \left[P_{H, Y}^V f_H^{0-} + P_{Hf, Y}^R \otimes f_{\sum_H f}^{0-} \right], \quad (\text{A.30})$$

where

$$f_{\sum_H f}^{0-} = f_{t_R}^{0-} - f_{q_L^3}^{0-}. \quad (\text{A.31})$$

- $\mathbf{T} = 1$ and $\text{CP} = +$:

$$\left[q \frac{\partial}{\partial q} f_{q_L^3}^{1+} \right]_Y = \frac{\alpha_Y}{\pi} \left[P_{q_L^3, Y}^V f_{q_L^3}^{1+} - N_c P_{fH, Y} \otimes f_H^{1+} \right] \quad (\text{A.32})$$

$$\left[q \frac{\partial}{\partial q} f_H^{1+} \right]_Y = \frac{\alpha_Y}{\pi} \left[P_{H, Y}^V f_H^{1+} - P_{Hf}^R \otimes f_{q_L^3}^{1+} \right] \quad (\text{A.33})$$

- $\mathbf{T} = 1$ and $\text{CP} = -$:

$$\left[q \frac{\partial}{\partial q} f_{t_L}^{1-} \right]_Y = \frac{\alpha_Y}{\pi} \left[P_{t_L, Y}^V f_{t_L}^{1-} + N_c P_{fH, Y} \otimes f_H^{1-} \right] \quad (\text{A.34})$$

$$\left[q \frac{\partial}{\partial q} f_H^{1-} \right]_Y = \frac{\alpha_Y}{\pi} \left[P_{H, Y}^V f_H^{1-} + P_{Hf, Y}^R \otimes f_{q_L^3}^{1-} \right] \quad (\text{A.35})$$

A.5 Mixed interaction

- $\mathbf{T} = 1$ and $\text{CP} = +$:

$$\left[q \frac{\partial}{\partial q} f_f^{1+} \right]_M = \frac{\alpha_M}{\pi} \frac{Y_f}{2} N_f P_{fV,G}^R \otimes f_{BW}^{1+}, \quad (\text{A.36})$$

$$\left[q \frac{\partial}{\partial q} f_{BW}^{1+} \right]_M = \frac{\alpha_M}{\pi} \left[4 \sum_{f_L} Y_f P_{fV,G}^R \otimes f_f^{1+} + 2 P_{VH,G}^R \otimes f_H^{1+} \right], \quad (\text{A.37})$$

$$\left[q \frac{\partial}{\partial q} f_H^{1+} \right]_M = \frac{\alpha_M}{\pi} \frac{1}{4} P_{HV,G}^R \otimes f_{BW}^{1+}, \quad (\text{A.38})$$

Equation (A.37) differs slightly from ref. [8] where, taking into account the definition there of $f_{B3} = f_{BW}/2$, an 8 would appear in place of 4 in the first term on the right-hand side.

Open Access. This article is distributed under the terms of the Creative Commons Attribution License ([CC-BY 4.0](https://creativecommons.org/licenses/by/4.0/)), which permits any use, distribution and reproduction in any medium, provided the original author(s) and source are credited.

References

- [1] A. Buckley et al., *General-purpose event generators for LHC physics*, *Phys. Rept.* **504** (2011) 145 [[arXiv:1101.2599](https://arxiv.org/abs/1101.2599)] [[INSPIRE](#)].
- [2] T. Sjöstrand, *A Model for Initial State Parton Showers*, *Phys. Lett.* **B 157** (1985) 321 [[INSPIRE](#)].
- [3] R.K. Ellis, W.J. Stirling and B.R. Webber, *QCD and collider physics*, *Camb. Monogr. Part. Phys. Nucl. Phys. Cosmol.* **8** (1996) 1 [[INSPIRE](#)].
- [4] J. Chen, T. Han and B. Tweedie, *Electroweak Splitting Functions and High Energy Showering*, [arXiv:1611.00788](https://arxiv.org/abs/1611.00788) [[INSPIRE](#)].
- [5] V.N. Gribov and L.N. Lipatov, *Deep inelastic $e p$ scattering in perturbation theory*, *Sov. J. Nucl. Phys.* **15** (1972) 438 [[INSPIRE](#)].
- [6] Y.L. Dokshitzer, *Calculation of the Structure Functions for Deep Inelastic Scattering and e^+e^- Annihilation by Perturbation Theory in Quantum Chromodynamics.*, *Sov. Phys. JETP* **46** (1977) 641 [[INSPIRE](#)].
- [7] G. Altarelli and G. Parisi, *Asymptotic Freedom in Parton Language*, *Nucl. Phys.* **B 126** (1977) 298 [[INSPIRE](#)].
- [8] P. Ciafaloni and D. Comelli, *Electroweak evolution equations*, *JHEP* **11** (2005) 022 [[hep-ph/0505047](https://arxiv.org/abs/hep-ph/0505047)] [[INSPIRE](#)].
- [9] H. Spiesberger, *QED radiative corrections for parton distributions*, *Phys. Rev.* **D 52** (1995) 4936 [[hep-ph/9412286](https://arxiv.org/abs/hep-ph/9412286)] [[INSPIRE](#)].
- [10] A.D. Martin, R.G. Roberts, W.J. Stirling and R.S. Thorne, *Parton distributions incorporating QED contributions*, *Eur. Phys. J.* **C 39** (2005) 155 [[hep-ph/0411040](https://arxiv.org/abs/hep-ph/0411040)] [[INSPIRE](#)].
- [11] M. Roth and S. Weinzierl, *QED corrections to the evolution of parton distributions*, *Phys. Lett.* **B 590** (2004) 190 [[hep-ph/0403200](https://arxiv.org/abs/hep-ph/0403200)] [[INSPIRE](#)].

- [12] NNPDF collaboration, R.D. Ball et al., *Parton distributions with QED corrections*, *Nucl. Phys. B* **877** (2013) 290 [[arXiv:1308.0598](#)] [[INSPIRE](#)].
- [13] R. Sadykov, *Impact of QED radiative corrections on Parton Distribution Functions*, [arXiv:1401.1133](#) [[INSPIRE](#)].
- [14] S. Carrazza, *Parton distribution functions with QED corrections*, [arXiv:1509.00209](#) [[INSPIRE](#)].
- [15] C. Schmidt, J. Pumplin, D. Stump and C.P. Yuan, *CT14QED parton distribution functions from isolated photon production in deep inelastic scattering*, *Phys. Rev. D* **93** (2016) 114015 [[arXiv:1509.02905](#)] [[INSPIRE](#)].
- [16] A. Manohar, P. Nason, G.P. Salam and G. Zanderighi, *How bright is the proton? A precise determination of the photon parton distribution function*, *Phys. Rev. Lett.* **117** (2016) 242002 [[arXiv:1607.04266](#)] [[INSPIRE](#)].
- [17] P. Ciafaloni and D. Comelli, *Sudakov enhancement of electroweak corrections*, *Phys. Lett. B* **446** (1999) 278 [[hep-ph/9809321](#)] [[INSPIRE](#)].
- [18] P. Ciafaloni and D. Comelli, *Electroweak Sudakov form-factors and nonfactorizable soft QED effects at NLC energies*, *Phys. Lett. B* **476** (2000) 49 [[hep-ph/9910278](#)] [[INSPIRE](#)].
- [19] M. Ciafaloni, P. Ciafaloni and D. Comelli, *Bloch-Nordsieck violating electroweak corrections to inclusive TeV scale hard processes*, *Phys. Rev. Lett.* **84** (2000) 4810 [[hep-ph/0001142](#)] [[INSPIRE](#)].
- [20] M. Ciafaloni, P. Ciafaloni and D. Comelli, *Electroweak double logarithms in inclusive observables for a generic initial state*, *Phys. Lett. B* **501** (2001) 216 [[hep-ph/0007096](#)] [[INSPIRE](#)].
- [21] M. Ciafaloni, P. Ciafaloni and D. Comelli, *Electroweak Bloch-Nordsieck violation at the TeV scale: ‘Strong’ weak interactions?*, *Nucl. Phys. B* **589** (2000) 359 [[hep-ph/0004071](#)] [[INSPIRE](#)].
- [22] M. Ciafaloni, P. Ciafaloni and D. Comelli, *Enhanced electroweak corrections to inclusive boson fusion processes at the TeV scale*, *Nucl. Phys. B* **613** (2001) 382 [[hep-ph/0103316](#)] [[INSPIRE](#)].
- [23] M. Ciafaloni, P. Ciafaloni and D. Comelli, *Towards collinear evolution equations in electroweak theory*, *Phys. Rev. Lett.* **88** (2002) 102001 [[hep-ph/0111109](#)] [[INSPIRE](#)].
- [24] P. Ciafaloni, D. Comelli and A. Vergine, *Sudakov electroweak effects in transversely polarized beams*, *JHEP* **07** (2004) 039 [[hep-ph/0311260](#)] [[INSPIRE](#)].
- [25] P. Ciafaloni and D. Comelli, *The Importance of weak bosons emission at LHC*, *JHEP* **09** (2006) 055 [[hep-ph/0604070](#)] [[INSPIRE](#)].
- [26] M. Ciafaloni, P. Ciafaloni and D. Comelli, *Electroweak double-logs at small x*, *JHEP* **05** (2008) 039 [[arXiv:0802.0168](#)] [[INSPIRE](#)].
- [27] P. Ciafaloni and A. Urbano, *Infrared weak corrections to strongly interacting gauge bosons scattering*, *Phys. Rev. D* **81** (2010) 085033 [[arXiv:0902.1855](#)] [[INSPIRE](#)].
- [28] P. Ciafaloni, D. Comelli, A. Riotto, F. Sala, A. Strumia and A. Urbano, *Weak Corrections are Relevant for Dark Matter Indirect Detection*, *JCAP* **03** (2011) 019 [[arXiv:1009.0224](#)] [[INSPIRE](#)].

- [29] S. Forte et al., *The Standard Model from LHC to future colliders*, *Eur. Phys. J. C* **75** (2015) 554 [[arXiv:1505.01279](#)] [[INSPIRE](#)].
- [30] M.L. Mangano et al., *Physics at a 100 TeV pp collider: Standard Model processes*, *CERN Yellow Report* (2017) 1 [[arXiv:1607.01831](#)] [[INSPIRE](#)].
- [31] J. Butterworth et al., *PDF4LHC recommendations for LHC Run II*, *J. Phys. G* **43** (2016) 023001 [[arXiv:1510.03865](#)] [[INSPIRE](#)].